Journal of Statistical Physics, Vol. 49, Nos. 5/6, 1987

Bethe Ansatz Calculations for the Eight-Vertex Model on a Finite Strip

Murray T. Batchelor,[1,4] Michael N. Barber,[2,5] and Paul A. Pearce[3]

Received May 18, 1987

Bethe ansatz equations for the eigenvalues of the transfer matrix of the eight-vertex model are solved numerically to yield mass gap data on infinitely long strips of up to 512 sites in width. The finite-size corrections, at criticality, to the free energy per site and polarization gap are found to be in agreement with recent studies of the XXZ spin chain. The leading corrections to the finite-size scaling estimates of the critical line and thermal exponent are also found, providing an explanation of the poor convergence seen in earlier studies. Away from criticality, the linear scaling fields are derived exactly in the full parameter space of the spin system, allowing a thorough test of a recently proposed method of extracting linear scaling fields and related exponents from finite lattice data.

KEY WORDS: Eight-vertex model; Bethe ansatz; finite-size scaling; scaling fields.

1. INTRODUCTION

The exact solution of many integrable models in statistical mechanics and field theory in one form or another involves the Bethe ansatz and its generalizations (see, e.g., Refs. 1–6). Generally, the Bethe ansatz equations constitute a set of transcendental equations whose solutions characterize a given eigenvalue and corresponding eigenvector of the transfer matrix or

[1] Department of Mathematics, The Faculties, Australian National University, Canberra, ACT, 2601, Australia.
[2] Institute for Theoretical Physics, University of California, Santa Barbara, California 93106.
[3] Department of Mathematics, University of Melbourne, Parkville, VIC, 3052, Australia.
[4] Present address: Instituut-Lorentz voor Theoretische Natuurkunde, 2311 SB Leiden, The Netherlands.
[5] Permanent address: Department of Mathematics, The Faculties, Australian National University, Canberra, ACT, 2601, Australia.

0022-4715/87/1200-1117$05.00/0

822/49/5-6-16

quantum Hamiltonian of the model. In the thermodynamic limit, the number of equations and solutions becomes infinite, but the equations can be transformed[1,4] to linear integral equations, which, at least for the dominant eigenvalues that are required for thermodynamic functions such as the free energy or surface tension, can be solved by the use of Fourier transform techniques.

Despite these successes of the Bethe ansatz in the thermodynamic limit, little use has been made, until recently, of the Bethe ansatz to evaluate quantities on *finite* lattices. This is somewhat surprising, since solution of the Bethe ansatz equations for a finite system could provide considerable information on the behavior of not only the finite system itself, but also of the bulk system. In particular, the critical behavior of the bulk system could be explored by finite-size scaling techniques (see, e.g., Ref. 7).

De Vega and Woynarovich[8] have recently developed a systematic procedure, based on the integral equation approach, for calculating the leading-order finite-size corrections for any model admitting a Bethe ansatz-type solution. This method was subsequently applied to the non-critical region of the XXZ Heisenberg chain.[8] Hamer[9,10] and Woynarovich and Eckle[11] have, however, shown how to extend the method to calculate finite-size corrections *at* criticality, and hence to infer critical exponents of the bulk XXZ system. Similar work has been reported for the XYZ chain[12] and the eight-vertex model.[13]

The method of de Vega and Woynarovich represents the solution of the Bethe ansatz equations for a large, finite system as a perturbation (by a sum of delta functions) of the density function that describes the solutions for the infinite lattice. An alternative approach to exploit the Bethe ansatz for a finite lattice is to solve directly the (finite) set of equations for the (finite) number of solutions characterizing the eigenvalues of the finite lattice theory. This is the approach we adopt here for the eight-vertex model; critical parameters are obtained by finite-size scaling techniques.

Several attempts at direct solution of the Bethe ansatz equations for a finite lattice have been reported for the isotropic Heisenberg chain. In particular, Grieger[14] and Borysowicz *et al.*[15] have computed ground-state correlation functions. Avdeev and Dörfel[16] have obtained the leading correction to the ground-state energy and explored the way in which the density of solutions approaches the bulk limit solution of the integral equation. Woynarovich and Eckle[11] have computed the lowest state in the two largest sectors of the critical XXZ chain, complementing their analytic analysis of the dominant finite-size corrections appearing in the model.

Recently Alcaraz *et al.*[17–19] have numerically solved the Bethe ansatz equations of the critical XXZ chain subject to periodic, "twisted," and free boundary conditions for several states as a means of calculating mass gap

amplitudes in the *critical* q-state Potts and Ashkin–Teller chains. This considerably extended the previous numerical estimates of bulk and surface exponents and allowed an examination of the dominant finite-size corrections appearing in the models.

In this paper, we directly solve the Bethe ansatz equations for the eight-vertex model. Our motivation, beyond the solution itself of the equations, is to explore the convergence of finite-size scaling and related techniques for this model. Early finite-size calculations[20-22] for the eight-vertex model were based on finite lattice data obtained by direct diagonalization of the transfer matrix in the spin formulation. As a result, eigenvalue data were restricted to strips of width up to 16 sites. While the estimates of bulk critical exponents were quite consistent with the exact results, several aspects warrant further investigation with data from larger lattices. Conventional phenomenological renormalization estimates converge well for small values of the four-spin coupling. However, the convergence deteriorates significantly as the four-spin coupling increases and indeed appears to become nonmonotonic. Data from large strips would clearly allow a nontrivial test of finite-size scaling and related techniques for a system with nonuniversal behavior.

The arrangement and content of this paper are as follows. In Section 2, we reformulate and examine the Bethe ansatz equations of the eight-vertex model. We then proceed to solve these equations numerically for the two simplest distributions of zeros. In Section 3 we define a mass gap from the corresponding eigenvalues and discuss the convergence rates of finite-size estimates of the critical line and thermal exponent. Finally, in Section 4 we derive exact expressions for the linear scaling fields in the full parameter space of the eight-vertex model. In this section we implement and fully test a recently proposed method[22,23] of extracting linear scaling fields from finite lattice data. The paper closes with a summary of our results.

2. THE BETHE ANSATZ EQUATIONS FOR THE EIGHT-VERTEX MODEL

2.1. Parametrization and Functional Equations

We begin by summarizing the results derived by Baxter[24,25] along with some caveats on the original notation. It is convenient numerically to work with the elliptic function

$$f(z, q) = \prod_{m=1}^{\infty} (1 - q^{m-1}z)(1 - q^m z^{-1})(1 - q^m) \tag{2.1a}$$

$$= \sum_{m=0}^{\infty} (-)^{m+1} q^{m(m+1)/2}(z^{m+1} - z^{-m}) \tag{2.1b}$$

where nome $q = e^{-\varepsilon}$, $\varepsilon = \pi I'/I$, with I and I' the complete elliptic integrals of the first kind. The usual elliptic theta functions $\Theta(z, q)$, $H(z, q)$, and $h(z, q) = \Theta(z, q)\, H(z, q)$ that appear in Baxter's formulation are related to this function by

$$\Theta(z, q) = f(qz, q^2), \qquad H(z, q) = iq^{1/4} z^{-1/2} f(z, q^2) \tag{2.2a}$$

$$h(z, q) = iq^{1/4} z^{-1/2} \frac{f^2(q^2, q^6)}{f(q, q^3)} f(z, q) \tag{2.2b}$$

Some useful properties of the elliptic function (2.1) are listed in Appendix A.

The connection between the spin and arrow formulations of the model was discovered originally by Wu[26] and Kadanoff and Wegner[27]; see also Baxter.[4] The allowed arrow configurations, along with one of the two equivalent sets of spin configurations, are shown in Fig. 1. Defining a set of spin couplings $\mathbf{K} = (K_1, K_1', K_2)$ as in Fig. 2, we obtain for the vertex weights

$$\begin{aligned} a &= R \exp(K_1 + K_1' + K_2), & b &= R \exp(-K_1 - K_1' + K_2) \\ c &= R \exp(K_1 - K_1' - K_2), & d &= R \exp(-K_1 + K_1' - K_2) \end{aligned} \tag{2.3}$$

where R is a normalization factor. In terms of the elliptic function defined in (2.1) these weights can be written as

$$\begin{aligned} a &= \frac{f(qx^{-1}z, q^2)\, f(qxz, q^2)}{f(q, q^2)\, f(qx^2, q^2)}, & b &= -\frac{q^{1/2} f(x^{-1}z, q^2)\, f(xz, q^2)}{z f(q, q^2)\, f(qx^2, q^2)} \\ c &= \frac{x^{1/2} f(qx^{-1}z, q^2)\, f(xz, q^2)}{z^{1/2} f(q, q^2)\, f(x^2, q^2)}, & d &= -\frac{x^{3/2} f(x^{-1}z, q^2)\, f(qxz, q^2)}{z^{1/2} f(q, q^2)\, f(x^2, q^2)} \end{aligned} \tag{2.4}$$

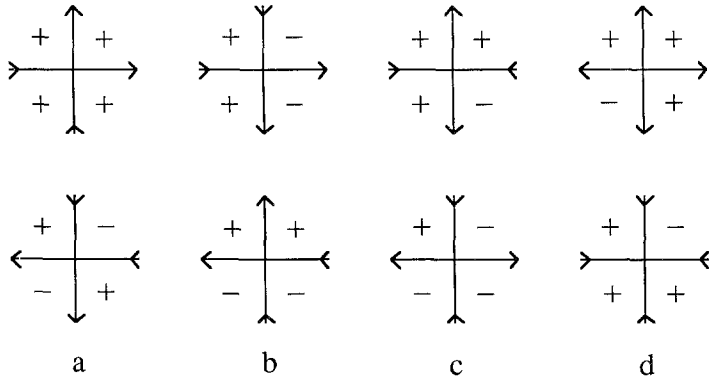

Fig. 1. The standard arrow and spin configurations of the eight-vertex model and their corresponding weights. An equivalent set of spin configurations has all spins reversed.

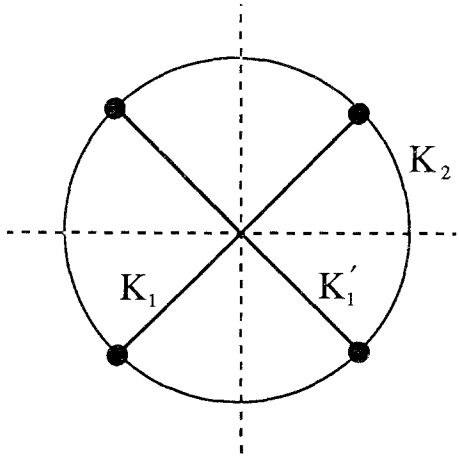

Fig. 2. Arrangement of spins (filled circles) and associated (reduced) coupling constants around a vertex.

where

$$z = \exp(i\pi v/I), \qquad x = \exp(i\pi\eta/I) \tag{2.5}$$

Since we will focus on the transition from the ferromagnetic ground state, we have rearranged the Baxter arrangement[28] of the weight parametrization. (The interchanges are $a \leftrightarrow c$, $b \leftrightarrow d$.) As a result, the critical line is given by

$$a = b + c + d \tag{2.6}$$

or

$$\sinh 2K_1 \sinh 2K_1' = \exp(-4K_2) \tag{2.7}$$

In the low-temperature (ferromagnetic) regime ($a > b + c + d$) we have

$$0 < q < x^2 < 1, \qquad x < z < x^{-1} \tag{2.8}$$

The symmetric case $K_1 = K_1'$ is given by $z = 1$, where $c = d$. The Ising limit $K_2 = 0$ is given by $q = x^4$, where $ab = cd$. The parametrization (2.4) is such that $q = 0$ at $T = 0$ and $q = 1$ at criticality.

All eigenvalues $T(z)$ of the row-to-row transfer matrix[24] are implicitly defined through the functional relation

$$(-)^{\nu' + \nu''} T(z)\, Q(z) = P(xz)\, Q(x^{-2}z) + P(x^{-1}z)\, Q(x^2 z) \tag{2.9a}$$

where

$$P(z) = \left[\frac{xf(z, q)}{z^{1/2} f(x^2, q)}\right]^N, \qquad N = 2n \tag{2.9b}$$

$$Q(z) = z^{-(n+v)/2} \prod_{j=1}^{n} f\left(\frac{z}{z_j}, q\right) \tag{2.9c}$$

Here N is the width of the strip.

The condition on the n zeros is

$$\left(\frac{1}{2} ivI' - \sum_{j=1}^{n} v_j\right) I^{-1} = n + v'' + \text{even integer} \tag{2.10}$$

which can also be written as

$$\prod_{j=1}^{n} z_j = (-)^{n+v''} q^{v/2} \tag{2.11}$$

The quantum numbers v' and v'' satisfy the following rules:

$v' = 0\ (1)$ if the number of down arrows in a row is even (odd)

$v'' = 0\ (1)$ if the corresponding eigenvector is symmetric (antisymmetric) with respect to arrow reversal.

A further quantum number v is defined via the condition

$$v + v' + n = \text{even integer} \tag{2.12}$$

implying that we can choose $v = v'$ for n even, and for n odd, v and v' to differ by one. For convenience, in all subsequent numerical computations we take n to be even, and thus N to be a multiple of four.

The generalized Bethe ansatz equations provide the zeros of the function $Q(z)$. These equations are obtained by setting $z = z_j$, $j = 1,..., n$, in Eq. (2.9a); the left-hand side vanishes, resulting in a set of n coupled nonlinear equations

$$\left[\frac{f(xz_j, q)}{f(x^{-1}z_j, q)}\right]^N = -x^{-2v} \prod_{k=1}^{n} \frac{f(x^2 z_j/z_k, q)}{f(x^{-2} z_j/z_k, q)}, \qquad j = 1,..., n \tag{2.13}$$

The logarithmic form of the eight-vertex equations has been discussed by Johnson *et al.*[29] (see also Takhtadzhan and Faddeev[30]). In our notation, we write the equations as

$$N\Phi_1(\phi_j) = -2\pi l_j - 2v \ln x + \sum_{k=1}^{n} \Phi_2(\phi_j - \phi_k), \qquad j = 1,..., n \tag{2.14}$$

where $z_j = \exp(i\phi_j)$. In (2.14) the l_j are half-integers and

$$\Phi_p(\phi) = \varphi(\phi, x^p) \tag{2.15}$$

where

$$\varphi(\phi, x) = -\pi - \phi - 2 \sum_{m=1}^{\infty} \frac{(x^m - x^{-m} q^m) \sin m\phi}{m(1-q^m)} \tag{2.16}$$

The function $\Phi_p(\phi)$ converges absolutely for q and x in the domain (2.8).

2.2. Solution on a Finite Lattice

Solutions of (2.13) and (2.14) are not known for general values of q, x, and n. Our interest in this paper is in the solutions corresponding to the two largest eigenvalues, from which we define a suitable mass gap. For even n, the maximum eigenvalue $T_0(z)$ has $v'' = 0$, while the next largest, $T_1(z)$, has $v'' = 1$. Both eigenvalues are in the sector with $v' = v = 0$.

2.2.1. Bootstrapping in Temperature

A first-order approximation valid for $q \ll x^2 \ll 1$ has been carried out by Baxter.[24] In this limit, (2.13) reduces to

$$z_j^n + (-)^{v''} = 0, \qquad j = 1, \ldots, n \tag{2.17}$$

i.e., the zeros characterizing $T_0(z)$ and $T_1(z)$ are the interlacing nth roots of $\pm$ unity. The corresponding limit in (2.14) indicates the following choice for the numbers l_j:

$$T_0(z): \quad l_j = j - 1/2, \qquad j = 1, \ldots, n \tag{2.18a}$$

$$T_1(z): \quad l_j = j + 1/2, \qquad j = 1, \ldots, n \tag{2.18b}$$

The distribution of zeros in the complex z plane for each eigenvalue is shown in Figs. 3a and 3c for $N = 32$. These zeros can be used as initial starting points in the numerical solution for either (2.13) or (2.14). Given a value of $x(\eta)$, the zeros are obtained by incrementing q and solving the thus modified set of equations for the new distribution of zeros. This distribution is used as input for another increment in q and so on. In this way we can "bootstrap" the zeros to their finite-temperature distributions. The zeros for $T_0(z)$ and $T_1(z)$ at $q = 0.1$ with $q = x^3$ ($\eta = iI'/3$) are shown in Figs. 3b and 3d. We observe that the sets of zeros remain interlaced.

The most convenient set of equations to solve numerically is the real system (2.14). In finding the n zeros we have used a standard library

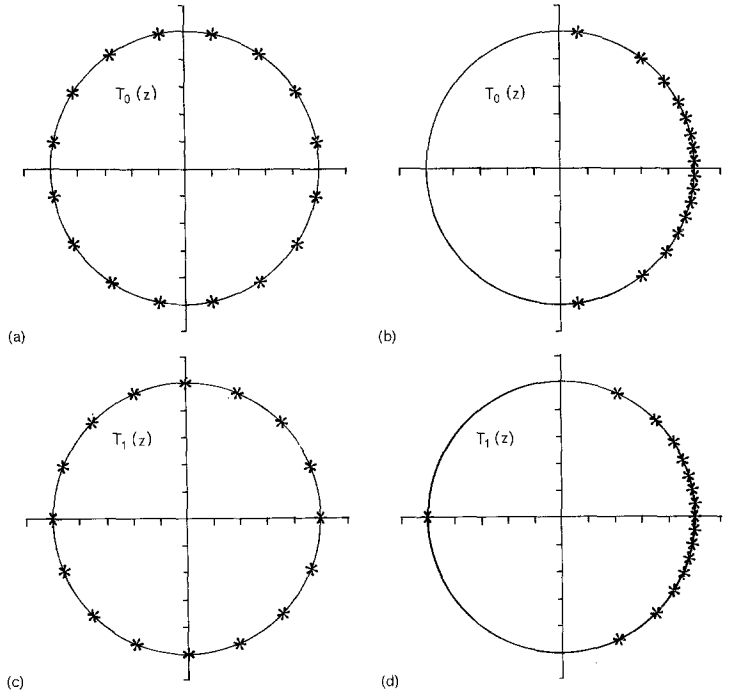

Fig. 3. Distributions of zeros on the unit circle in the complex z plane for eigenvalues $T_0(z)$ and $T_1(z)$ on a strip of width $N=32$. (a, c) Distributions at $q=0$. (b, d) Distributions at $q=0.1$ with $\eta=iI'/3$ ($q=x^3$).

package[31] implementing a Newton-type method. We have checked, for lattice sizes $N=4$ and $N=8$, the eigenvalues obtained in this way with the results of a "brute-force" diagonalization of the transfer matrix. In practice, as the zeros z_j occur in complex conjugate pairs, the number of zeros and equations can be reduced to $n/2$ for $T_0(z)$ and $n/2-1$ for $T_1(z)$, where we further factor out the stationary zeros at $\phi_1=0$ and $\phi_n=\pi$.

2.2.2. Exact Solutions in the Ising Limit

As an alternative to bootstrapping from the low-temperature limit, for a given value of q, the incremention can be in the variable x away from the exact Ising solutions. When $q=x^4$ ($\eta=iI'/4$), the Bethe ansatz equations decouple and the solutions can be written in closed form. The simplest approach is via (2.14), which reduces to

$$N\Phi_1(\phi)=-2\pi l_j-n(\pi+\phi_j)+\sum_{k=1}^{n}\phi_k, \qquad j=1,\ldots,n \tag{2.19}$$

On rearranging, this can be written as

$$\frac{2\pi}{N} l_j - \frac{\pi}{2} - \frac{1}{N} \sum_{k=1}^{n} \phi_k = \mathrm{am}\left(\frac{\tilde{I}\phi_j}{\pi}, \tilde{k}\right) \tag{2.20}$$

where $\mathrm{am}(u, k)$ is the elliptic amplitude function of argument u and modulus k (see, e.g., Gradshteyn and Ryzhik[32]) satisfying

$$u = \mathscr{F}(\mathrm{am}(u, k), k) \tag{2.21a}$$

with $\mathscr{F}(\theta, k)$ the elliptic integral of the first kind:

$$\mathscr{F}(\theta, k) = \int_0^{\theta} \frac{d\alpha}{(1 - k^2 \sin^2 \alpha)^{1/2}} \tag{2.21b}$$

In (2.20), the modulus $\tilde{k}$ is defined by

$$\tilde{I}'/\tilde{I} = \tfrac{1}{4} I'/I \tag{2.22}$$

with associated nome $\tilde{q} = x$ (recall $q = x^4$). From (2.20) and (2.21) we obtain the following solutions:

$$T_0(z): \quad \phi_j = \frac{\pi}{\tilde{I}} \mathscr{F}\left(\frac{2\pi}{N} l_j - \frac{\pi}{2}, \tilde{k}\right), \qquad j = 1, \ldots, n \tag{2.23a}$$

$$T_1(z): \quad \phi_j = \frac{\pi}{\tilde{I}} \mathscr{F}\left(\frac{2\pi}{N} l_j - \frac{\pi}{2} - \frac{\pi}{N}, \tilde{k}\right), \qquad j = 1, \ldots, n \tag{2.23b}$$

In practice, to evaluate these zeros we first compute $\tilde{k}$ and $\tilde{I}$ using the formulas[32]

$$\tilde{I} = \frac{\pi}{2}\left(1 + 2 \sum_{m=1}^{\infty} x^{m^2}\right)^2 \tag{2.24}$$

$$\tilde{k} = \frac{2\pi}{\tilde{I}} x^{1/2} \left[\sum_{m=1}^{\infty} x^{m(m-1)}\right]^2 \tag{2.25}$$

2.2.3. Initial Approximation of Zeros

For the largest eigenvalue, an initial approximation to the zeros for any values of q and x, increasing in accuracy with system size, can be obtained by generalizing[18] the method outlined by Grieger[14] in the computation of the ground state of the isotropic XXZ antiferromagnet. Here we appropriately sample the known[29,30] distribution of zeros for $T_0(z)$ to

provide approximations to the zeros of both leading eigenvalues. To derive the necessary result, we follow Hamer[13] and introduce the quantity

$$Z_N(\phi) = -\frac{1}{2\pi}\left[\Phi_1(\phi) - \frac{1}{N}\sum_{k=1}^{n}\Phi_2(\phi_j - \phi_k)\right] \tag{2.26}$$

so that, from (2.14), at the zeros ϕ_j we have

$$Z_N(\phi_j) = l_j/N \tag{2.27}$$

Defining

$$R_N(\phi) = \frac{dZ_N(\phi)}{d\phi} \tag{2.28}$$

gives[29,30]

$$R_\infty(\phi) = \frac{1}{4\pi}\sum_{m=-\infty}^{\infty}\frac{\exp(im\phi)}{\cosh m\lambda} = \frac{\tilde{I}}{2\pi^2}\,\mathrm{dn}\left(\frac{\tilde{I}\phi}{\pi}, \tilde{k}\right) \tag{2.29}$$

where $\mathrm{dn}(u, k)$ is a standard elliptic function.[32] In (2.29), the modulus $\tilde{k}$ is defined by

$$\tilde{I}'/\tilde{I} = \lambda/\pi = -i\eta/I \tag{2.30}$$

with associated nome $\tilde{q} = x$. Using Eqs. (2.28) and (2.29), we have

$$Z_\infty(\phi) = (1/2\pi)\,\mathrm{am}(\tilde{I}\phi/\pi, \tilde{k}) \tag{2.31}$$

Finally, from Eqs. (2.21), (2.27), and (2.31),

$$\phi_j = \frac{\pi}{\tilde{I}}\mathscr{F}\left(\frac{2\pi}{N}l_j, \tilde{k}\right) \tag{2.32}$$

should be a good approximation to the zeros ϕ_j, becoming exact as $N \to \infty$. Realize, however, that (2.32) is the result (2.23a) obtained in the Ising case. Both of the Ising results (2.23a) and (2.23b) are thus excellent approximation formulas for all values of q and x. In Table I the values obtained from these formulas for $q = x^3 = 0.1$ and $N = 32$ are compared with the exact numerical results. As can be seen, the agreement is close, resulting in rapid convergence to the exact zeros.

2.3. Comparison with Bulk Results

For the symmetric case ($z = 1$), (2.9a) simplifies to give the largest eigenvalue in the form

$$T_0(1) = 2\left[\frac{f(x, q)}{f(x^2, q)}\right]^N \prod_{j=1}^{n}\frac{f(x^2 z_j, q)}{f(z_j, q)} \tag{2.33}$$

Table I. Approximate and Exact (Numerical) Zeros Φ_j Characterizing the Eigenvalues $T_0(z)$ and $T_1(z)$ on a Strip of Width $N=32$ for $\eta=iI'/3$ ($q=x^3$) and $q=0.1$

$T_0(z)$		$T_1(z)$	
Approximate	exact	Approximate	exact
0.048047	0.048023	0.096562	0.096609
0.146037	0.145959	0.197011	0.197114
0.250106	0.249957	0.306071	0.306257
0.365844	0.365583	0.430653	0.430980
0.502181	0.501708	0.582855	0.583482
0.676405	0.675428	0.789042	0.790538
0.932371	0.929549	1.132394	1.139276
1.471868	1.446502		

where we have exploited the fact that the zeros occur in unimodular complex conjugate pairs. However, for $v''=1$, (2.9a) reduces to the identity "zero = zero." To obtain an expression for $T_1(1)$, we differentiate (2.9a) with respect to z and *then* set $z=1$. The result is

$$T_1(1)=-\left[\frac{f(x,q)}{f(x^2,q)}\right]^N \frac{f(x^2,q)}{g(1,q)} F(x,q) \prod_{j=2}^{n} \frac{f(x^2 z_j, q)}{f(z_j, q)} \tag{2.34a}$$

in which

$$F(x,q)=\sum_{j=1}^{n}\left[\frac{g(x^{-2}z_j^{-1},q)}{f(x^2 z_j,q)}-\frac{g(x^2 z_j^{-1},q)}{f(x^{-2}z_j,q)}\right] - \frac{N}{f(x,q)}\left[g(x^{-1},q)+xg(x,q)\right] \tag{2.34b}$$

where

$$g(z,q)=\frac{d}{dz}f(z,q) \tag{2.35}$$

and in (2.34) $z_1=1$. There are *no* such cancellation problems in the nonsymmetric case.

Given $T_0(z)$ and $T_1(z)$, the free energy per site f_N and the interfacial tension σ_N can be defined on a strip of width N as[4]

$$-\beta f_N=\frac{1}{N}\ln T_0(z) \tag{2.36}$$

$$-\beta\sigma_N=\frac{1}{N}\ln\ln\frac{T_0(z)}{T_1(z)} \tag{2.37}$$

The exact results derived by Baxter,[24,28,4] valid in the thermodynamic limit, are

$$-\beta f_\infty = \ln a + \sum_{m=1}^{\infty} \frac{(x^m + x^{-m} - z^m - z^{-m})(x^{2m} - q^m)^2}{m x^m (1-q^{2m})(1+x^{2m})} \tag{2.38}$$

$$-\beta\sigma_\infty = \frac{1}{2}\ln\left[4x \prod_{m=1}^{\infty}\left(\frac{1+x^{4m}}{1+x^{4m-2}}\right)^4\right] \tag{2.39}$$

In Table II we show the values of (2.36) and (2.37) for $z=1$, $q=x^3=0.1$, and $q=x^6=0.01$ on finite strips of width $N=2^m$, $m=2, 3,\ldots, 8$. For comparison we also list the bulk limits given in (2.38) and (2.39). The slow convergence of the interfacial tension is presumably a result of the double logarithm in its definition.

It should be noted that the only real limit imposed on the evaluation of $T_0(z)$ and $T_1(z)$ with increasing system size is in the resolution of zeros as q tends to its critical value (as can be seen from Figs. 3b and 3d, the nonstationary zeros will coalesce at $z=1$ in this limit). For this reason, to examine the critical region in detail, we derive an alternative parametrization of the vertex weights (2.4) and the functional equation (2.9).

2.4. Reformulation at Criticality

The limit $q \to 1$ can be handled by using the conjugate nome identities outlined in Appendix B. In terms of the conjugate variables

$$\zeta = \exp(iw), \qquad \chi = \exp(i\mu), \qquad p = \exp(-2\pi^2/\varepsilon) \tag{2.40}$$

Table II. Finite Lattice Estimates (2.36) and (2.37) of the Eight-Vertex Model Free-Energy per Site and Interfacial Tension[a]

	$q=x^3=0.1$			$q=x^6=0.01$		
N	$-\beta f_N^{(0)}$	$-\beta f_N^{(1)}$	$-\beta\sigma_N$	$-\beta f_N^{(0)}$	$-\beta f_N^{(1)}$	$-\beta\sigma_N$
4	0.335068	0.274637	0.3550	0.111023	−0.005419	0.1910
8	0.311680	0.295782	0.2578	0.088066	0.059143	0.1830
16	0.305641	0.301653	0.1720	0.082064	0.075222	0.1383
32	0.304114	0.303143	0.1085	0.080553	0.079016	0.0941
64	0.303732	0.303507	0.0663	0.080181	0.079862	0.0608
128	0.303638	0.303592	0.0401	0.080092	0.080035	0.0385
256	0.303616	0.303609	0.0248	0.080073	0.080066	0.0245
∞	0.303612...		0.0064...	0.080069...		0.0064...

[a] Also shown is the quantity $-\beta f_N^{(1)} = N^{-1}\ln T_1(z)$.

with $w = -i2\pi v/I'$ and $\mu = -i2\pi\eta/I'$ the vertex weights (2.4) can be written as

$$a = \rho(\chi\zeta^{-1})^{1/2}\frac{f(-(\chi\zeta)^{1/2}, p)\, f(-(\chi^{-1}\zeta)^{1/2}, p)}{f(-\chi, p)\, f(-1, p)} \tag{2.41a}$$

$$b = \rho(\chi\zeta^{-1})^{1/2}\frac{f((\chi\zeta)^{1/2}, p)\, f((\chi^{-1}\zeta)^{1/2}, p)}{f(-\chi, p)\, f(-1, p)} \tag{2.41b}$$

$$c = \rho(\chi\zeta^{-1})^{1/2}\frac{f((\chi\zeta)^{1/2}, p)\, f(-(\chi^{-1}\zeta)^{1/2}, p)}{f(\chi, p)\, f(-1, p)} \tag{2.41c}$$

$$d = -\rho(\chi\zeta^{-1})^{1/2}\frac{f(-(\chi\zeta)^{1/2}, p)\, f((\chi^{-1}\zeta)^{1/2}, p)}{f(\chi, p)\, f(-1, p)} \tag{2.41d}$$

The normalization factor ρ is given by

$$\rho = \exp[(\pi/2II')(\eta^2 - v^2)] \tag{2.42}$$

In the ferromagnetic regime, the new variables (2.40) satisfy

$$|z| = |\chi| = 1, \qquad 0 < p < 1, \qquad |w| < \mu < \pi \tag{2.43}$$

and the square root is taken so that

$$-\pi/2 < \arg(\zeta^{1/2}) \leqslant \pi/2 \tag{2.44}$$

The functional equation (2.9) transforms to

$$(-)^{\nu' + \nu''} T(\zeta)\, Q(\zeta) = P(\chi\zeta)\, Q(\chi^{-2}\zeta) + P(\chi^{-1}\zeta)\, Q(\chi^2\zeta) \tag{2.45a}$$

with

$$P(\zeta) = \left[\rho\frac{\chi}{\sqrt{\zeta}}\frac{f(\zeta, p^2)}{f(\chi^2, p^2)}\right]^N \tag{2.45b}$$

$$Q(\zeta) = \zeta^{-(\nu'' + n + e\nu)/2}\prod_{j=1}^{n} f\left(\frac{\zeta}{\zeta_j}, p^2\right) \tag{2.45c}$$

Finally, the condition on the zeros (2.10) reads

$$\prod_{j=1}^{n}\zeta_j = (-)^{\nu}\, p^{\nu'' + n + e\nu} \tag{2.46}$$

The symmetric case ($K_1 = K_1'$) is now given by $w = 0$ and the Ising limit ($\eta = iI'/4$) by $\mu = \pi/2$. Duality is given by the simple interchange

$p \leftrightarrow -p$, criticality occurring at $p=0$. From (2.45a) the zeros specifying a given eigenvalue are now solutions of

$$\left[\frac{f(\chi\zeta_j, p^2)}{f(\chi^{-1}\zeta_j, p^2)}\right]^N = -\chi^{-2v''} \prod_{k=1}^{n} \frac{f(\chi^2\zeta_j\zeta_k^{-1}, p^2)}{f(\chi^{-2}\zeta_j\zeta_k^{-1}, p^2)}, \qquad j=1,\ldots,n \tag{2.47}$$

where, for n even, we have chosen $ev=-n$. For the symmetric case, the analogous relations to (2.33) and (2.34) are

$$T_0(1) = 2\left[\rho\frac{f(\chi, p^2)}{f(\chi^2, p^2)}\right]^N \prod_{j=1}^{n} \frac{f(\chi^2\zeta_j, p^2)}{f(\zeta_j, p^2)} \tag{2.48}$$

$$T_1(1) = -\left[\rho\frac{f(\chi, p^2)}{f(\chi^2, p^2)}\right]^N \chi F(\chi, p^2)\frac{f(\chi^2, p^2)}{g(1, p^2)} \prod_{j=2}^{n} \frac{f(\chi^2\zeta_j, p^2)}{f(\zeta_j, p^2)} \tag{2.49}$$

in which $F(\chi, p^2)$ is as defined in (2.34b), only now with z_j, x, and q replaced by ζ_j, χ, and p^2. Here the zeros $z_1=1$ and $z_2=-1$ map to the values $\zeta_1=1$ and $\zeta_2=p$.

In deriving a logarithmic form of Eqs. (2.47), it is convenient to consider separately the zeros for $T_0(\zeta)$ and $T_1(\zeta)$.

2.4.1. Zeros for $T_0(\zeta)$

On setting $\zeta_j=\exp(-2\alpha_j)$ and using the definition (2.1), we can write, for example,

$$\frac{f(\chi\zeta_j, p^2)}{f(\chi^{-1}\zeta_j, p^2)} = e^{i\mu}\frac{\sinh(\alpha_j - i\mu/2)}{\sinh(\alpha_j + i\mu/2)} \prod_{m=1}^{\infty} \frac{1+p^{4m}-p^{2m}\cosh(2\alpha_j - i\mu)}{1+p^{4m}-p^{2m}\cosh(2\alpha_j + i\mu)} \tag{2.50}$$

Subsequently on taking logarithms in (2.47) we introduce the quantities φ and Φ defined by

$$\exp(i\varphi) \equiv -\frac{\sinh(\alpha - i\mu/2)}{\sinh(\alpha + i\mu/2)} \tag{2.51}$$

$$\exp(i\Phi) \equiv \frac{1+p^2+2p\cosh(2\alpha - i2\mu)}{1+p^2-2p\cosh(2\alpha + i2\mu)} \tag{2.52}$$

with

$$\varphi(\alpha, \mu) = 2\tan^{-1}(\cot\mu\tanh\alpha) \tag{2.53}$$

$$\Phi(\alpha, \mu, p) = 2\tan^{-1}\left(\frac{2p\sinh 2\alpha \sin 2\mu}{1+p^2-2p\cosh 2\alpha\cos 2\mu}\right) \tag{2.54}$$

For $T_0(\zeta)$ the Bethe ansatz equations can then be written in the form

$$N\Psi(\alpha_j, \mu/2) = 2\pi I_j + \sum_{k=1}^{n} \Psi(\alpha_j - \alpha_k, \mu), \qquad j = 1,..., n \tag{2.55}$$

where

$$\Psi(\alpha, \mu) = \varphi(\alpha, \mu) + \sum_{m=1}^{\infty} \Phi(\alpha, \mu, p^{2m}) \tag{2.56}$$

and the I_j are half-integers given by

$$I_j = (2j - n - 1)/2, \qquad j = 1,..., n \tag{2.57}$$

2.4.2. Zeros for $T_1(\zeta)$

The zero $\zeta_1 = p$ trivially satisfies the first of the equations (2.47). On relabeling, the remaining $n-1$ zeros satisfy

$$\left[\frac{f(\chi\zeta_j, p^2)}{f(\chi^{-1}\zeta_j, p^2)}\right]^N = -\chi^2 \frac{f(p\chi^2\zeta_j, p^2)}{f(p\chi^{-2}\zeta_j, p^2)} \times \prod_{k=1}^{n-1} \frac{f(\chi^2\zeta_j\zeta_k^{-1}, p^2)}{f(\chi^{-2}\zeta_j\zeta_k^{-1}, p^2)}, \qquad j = 1,..., n-1 \tag{2.58}$$

and subsequently, on taking logarithms,

$$N\Psi(\alpha_j, \mu/2) = 2\pi I_j + \sum_{m=1}^{\infty} \Phi(\alpha_j, \mu, p^{2m-1}) + \sum_{k=1}^{n-1} \Psi(\alpha_j - \alpha_k, \mu), \qquad j = 1,..., n-1 \tag{2.59}$$

with integers I_j given by

$$I_j = j - n + 2, \qquad j = 1,..., n-1 \tag{2.60}$$

2.4.3. Approximation of Zeros

Rather than repeating the working in Section 2.2 and inverting appropriate elliptic functions, the shortest path to the desired formula is the direct transformation of the final result (2.32). Using the identity

$$\frac{\tilde{I}}{I} = \frac{2\pi}{\mu}\frac{\tilde{I}'}{I'} \tag{2.61}$$

we can use (2.32) to write

$$\alpha_j = \frac{\mu}{2\tilde{I}'} \mathscr{F}\left(\frac{2\pi}{N} I_j, (1-\tilde{k}'^2)^{1/2}\right) \tag{2.62}$$

with nome $\tilde{q}' = p^{\pi/\mu}$. The zeros (2.62) now provide excellent initial approximations to the zeros of the systems (2.55) and (2.59).

2.5. Bethe Ansatz Equations and Eigenvalues at Criticality

At $p=0$, Eqs. (2.55), with the choice of the numbers I_j in (2.57), reduce to the Bethe ansatz equations describing the leading eigenvalue of either the six-vertex model or the XXZ chain.[1,4] Correspondingly, Eqs. (2.59) with (2.60) describe the leading eigenvalue in the next largest sector of either model. Defining

$$\alpha_j = \tanh^{-1}(\tan \tfrac{1}{2}\mu \tan \tfrac{1}{2}\theta_j) \tag{2.63}$$

we can write the equations for $T_0(\zeta)$ and $T_1(\zeta)$ as

$$N\theta_j = 2\pi I_j - \sum_{k=1}^{r} \Theta(\theta_j, \theta_k), \qquad j = 1,..., r \tag{2.64}$$

where

$$\Theta(\theta, \theta') = 2\tan^{-1}\left[\frac{\Delta \sin \frac{1}{2}(\theta-\theta')}{\cos \frac{1}{2}(\theta+\theta') - \Delta \cos \frac{1}{2}(\theta-\theta')}\right] \tag{2.65}$$

in which we make the identification $\Delta = -\cos\mu$. In (2.64), $r=n$ for $T_0(\zeta)$ and $r=n-1$ for $T_1(\zeta)$.

Finally, for $p=0$, (2.62) can be evaluated explicitly to give

$$\alpha_j = \frac{\mu}{\pi} \ln \tan \pi\left(\frac{I_j}{N} + \frac{1}{4}\right) \tag{2.66}$$

This last approximation formula was used by Alcaraz *et al.*[18] in their discussion of the numerical solution of the XXZ Bethe ansatz equations. In this limit the expressions for the two largest eigenvalues, (2.48) and (2.49), reduce to

$$T_0(1) = 2\left[\frac{\rho}{2\cos(\mu/2)}\right]^N \prod_{j=1}^{n/2} \frac{\cosh 2\alpha_j - \cos 2\mu}{\cosh 2\alpha_j - 1} \tag{2.67}$$

$$T_1(1) = 2E\left[\frac{\rho}{2\cos(\mu/2)}\right]^N \prod_{j=1}^{n/2-1} \frac{\cosh 2\alpha_j - \cos 2\mu}{\cosh 2\alpha_j - 1} \tag{2.68}$$

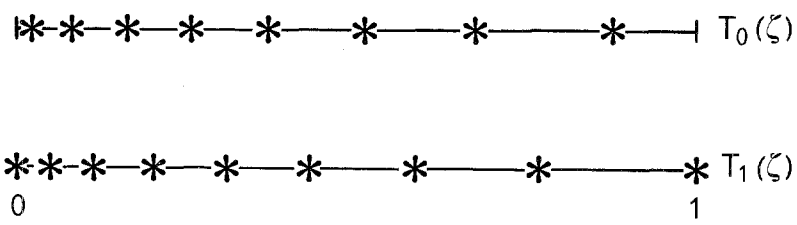

Fig. 4. Critical distributions of zeros on the real axis in the complex ζ plane for eigenvalues $T_0(\zeta)$ and $T_1(\zeta)$ on a strip of width $N=32$ with $\eta = iI'/3$ ($\mu = 2\pi/3$). Each zero on the open interval (0, 1) has a reciprocal on (1, ∞).

where

$$E = 2N\cos^2\frac{\mu}{2} - \cos\mu - \sum_{j=1}^{n/2-1} \frac{2\sin\mu\sin 2\mu}{\cosh 2\alpha_j - \cos 2\mu} \tag{2.69}$$

Here we have written the eigenvalues in terms of the zeros on (0, ∞), which we can solve for separately[18] (see also Appendix D).

In Fig. 4 we show the zeros ζ_j characterizing the eigenvalues $T_0(\zeta)$ and $T_1(\zeta)$ at criticality. In the limit $p=1$ all of the zeros are at the point $\zeta = 1$. As p decreases, apart from the stationary zero at $\zeta = 1$, the zeros all move smoothly to the left until at criticality they occupy the positions shown in the figure.

3. FINITE-SIZE SCALING

The numerical solution of the eight-vertex-model Bethe-ansatz equations described in the preceding section allows the mass gap

$$\kappa_N = \ln(T_0/T_1) \tag{3.1}$$

to be easily evaluated for strips us to $N \approx 256$ for general couplings and up to $N \approx 512$ at criticality. These values of N far exceed the lattice sizes ($N \sim 16$) available in previous lattice studies of the eight-vertex model.[20–22] As mentioned in the Introduction, this allows a nontrivial test of finite-size scaling and a detailed investigation of *convergence* rates.[33,7] We begin by considering the free energy and mass gap *at* criticality, for which the expected behavior is predicted by conformal invariance.[34]

3.1. Free Energy at Criticality

For a finite strip with periodic boundary conditions, conformal invariance predicts[35,36] the free energy per site f_N to approach its limiting value f_∞ as

$$f_N = f_\infty - \tfrac{1}{6}\pi c N^{-2} + o(N^{-2}) \tag{3.2}$$

where c is the conformal anomaly. For a model with a line of continuously varying exponents c is expected to be unity.[37] This prediction has been tested by Blöte *et al.*,[35] using data from strips of up to 16 sites. Excellent agreement was found for $-0.3 < K_2 \leqslant 0.4$ ($0.3 < \mu/\pi \leqslant 0.7$), but for K_2 outside this range the convergence deteriorated significantly.

From (2.36) and (2.67), the free energy of the eight-vertex model on a finite strip is

$$-\beta f_N = \ln\left(\frac{\rho}{2\cos(\mu/2)}\right) + \frac{1}{N}\left(\ln 2 + \sum_{j=1}^{n/2} \ln\frac{\cosh 2\alpha_j - \cos 2\mu}{\cosh 2\alpha_j - 1}\right) \tag{3.3}$$

Taking the thermodynamic limit, we have[1,4]

$$-\beta f_\infty = \ln\left(\frac{\rho}{2\cos(\mu/2)}\right) + \int_{-\infty}^{\infty} \frac{d\alpha}{4\mu\cosh(\pi\alpha/\mu)} \ln\frac{\cosh 2\alpha - \cos 2\mu}{\cosh 2\alpha - 1} \tag{3.4a}$$

The integral appearing in this result also occurs in the exact solution of the F model[1] and has been tabulated by Temperley and Lieb[38] for several values of $\cos\mu$. In particular, at $\mu = \pi/3$, $\pi/2$, and $2\pi/3$, the exact[38] results are, respectively, $\ln 2$, $2/\pi \times$ Catalan's constant, and $3/2\ln(4/3)$. As pointed out by Temperley and Lieb, however, the integral is awkward to evaluate numerically because of the logarithmic singularity at $\alpha = 0$. In our case, it is more convenient to use the result[24,4]

$$-\beta f_\infty = \ln\left(\frac{\rho}{\cos(\mu/2)}\right) + \int_{-\infty}^{\infty} \frac{\{\cosh[(\pi - 2\mu)t] - \cosh\mu t\}(\cosh\mu t - 1)}{2t\sinh\pi t\cosh\mu t}\, dt \tag{3.4b}$$

To estimate c, we define estimators

$$c_N = \frac{6}{\pi}[f_\infty - f_N]\, N^2 \tag{3.5}$$

which, from (3.2), should tend to $c = 1$ as $N \to \infty$. In Table III we show the sequence (3.5) for $N = 2^m$, $m = 2, 3, \ldots, 9$, at several values of μ. For all values of μ, the estimates are clearly seen to approach the value $c = 1$ as N increases. The convergence does appear to be slower, however, for μ less than $\pi/3$. We note also that the convergence is nonmonotic for $\mu = \pi/6$ and $\pi/12$.

Table III. Finite Lattice Estimates (3.5) of the Conformal Anomaly ($c=1$) of the Eight-Vertex Model As a Function of the Parameter μ

N	$\mu=\pi/12$	$\mu=\pi/6$	$\mu=\pi/3$	$\mu=\pi/2$	$\mu=2\pi/3$	$\mu=5\pi/6$	$\mu=11\pi/12$
4	0.957470	0.956599	0.949226	0.942761	0.961539	1.361967	2.462339
8	0.992158	0.991221	0.985873	0.983256	0.987381	1.111180	2.260590
16	1.000772	0.999861	0.996486	0.995589	0.996591	1.012555	1.359595
32	1.001997	1.001164	0.999164	0.998881	0.999130	1.002391	1.030141
64	1.001691	1.000959	0.999804	0.999719	0.999781	1.000572	1.005016
128	1.001239	1.000616	0.999954	0.999930	0.999945	1.000142	1.001205
256	1.000886	1.000367	0.999990	0.999982	0.999986	1.000035	1.000299
512	1.000638	1.000213	0.999998	0.999996	0.999997	1.000009	1.000075

To quantify the convergence rate, we assume

$$c_N = 1 + aN^{-\lambda}, \qquad N \to \infty \tag{3.6}$$

and define estimators

$$L_m = \frac{\ln[(c_{2^m}-1)/(c_{2^{m+1}}-1)]}{\ln 2} \to \lambda \qquad \text{as} \quad m \to \infty \tag{3.7}$$

This sequence converges rapidly with increasing m; in Fig. 5 we show the estimator L_8 as a function of μ together with the value

$$\lambda = \begin{cases} 4\mu/(\pi-\mu), & 0<\mu<\pi/3 \\ 2, & \pi/3<\mu<\pi \end{cases} \tag{3.8}$$

which appears to account for the observed convergence over the whole range except at $\mu=\pi/3$. The value, (3.8), also agrees with the result obtained for the XXZ chain.[17,18,10,11] For $\mu=\pi/3$, as in the XXZ chain, we find that the convergence can be accounted for by assuming that $c_N \approx 1 + O[(\ln N)/N^2]$, where the amplitude is estimated to be approximately 0.83. The physical significance of these results will be discussed in Section 3.5.

3.2. Mass Gap Amplitude at Criticality

Turning now to the mass gap, (3.1), we expect that at criticality[34]

$$N\kappa_N = 2\pi x_p + o(1) \qquad \text{as} \quad N \to \infty \tag{3.9}$$

where x_p is the anomalous dimension of the operator linking the two states $|0\rangle$ and $|1\rangle$. Since we are working in the arrow formulation of the eight-

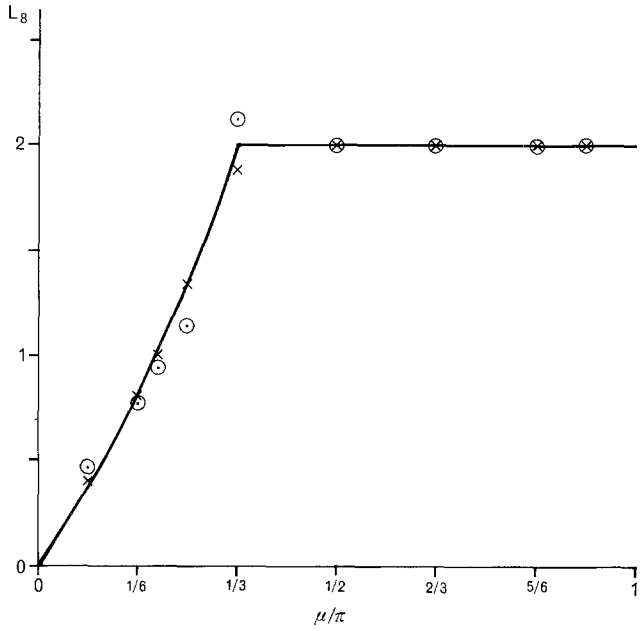

Fig. 5. The (negated) exponent of the leading correction to the conformal anomaly estimates (3.6) and the polarization mass gap (3.9) as a function of μ. The estimators L_8 [Eq. (3.7)] are indicated by the dotted circles, while crosses indicate the corresponding estimate for the mass gap (3.9). The anomalous convergence at $\mu = \pi/3$ can be attributed to a logarithmic correction (see text).

vertex model, this operator is associated with the polarization and hence we expect

$$x_p = (\pi - \mu)/2\pi \tag{3.10}$$

This result was first established by Nightingale and Blöte,[39] using strips of up to 16 sites. Again, poor convergence was observed at both extremes of K_2 (this is particularly evident in Nightingale and Blöte's Figure 1c). The result is further supported by the values in Table IV. The corresponding states in the XXZ chain (i.e., states characterized by the same Bethe ansatz zeros), not surprisingly, yield the same exponent.[18] The results of a similar analysis as described above for c to quantify the convergence in (3.9) are shown in Fig. 5, also from strips of width $N = 256$ and 512. The leading correction to (3.9) is again proportional to $N^{-\lambda}$ with λ given by (3.8). Again at $\mu = \pi/3$, the correction is logarithmic, of order $(\ln N)/N^2$.

Table IV. Finite Lattice Estimates $N\kappa_N/2\pi$ of the Anomalous Dimension x_p of the Eight-Vertex Model Polarization Operator As a Function of the Parameter μ

N	$\mu=\pi/12$	$\mu=\pi/6$	$\mu=\pi/3$	$\mu=\pi/2$	$\mu=2\pi/3$	$\mu=5\pi/6$	$\mu=11\pi/12$
4	0.388924	0.373731	0.317639	0.239657	0.154393	0.063194	0.019819
8	0.414303	0.394662	0.328363	0.246999	0.163237	0.078204	0.031844
16	0.428880	0.405138	0.331895	0.249212	0.165774	0.082220	0.039639
32	0.437706	0.410434	0.332933	0.249800	0.166441	0.083060	0.041346
64	0.443422	0.413217	0.333223	0.249950	0.166610	0.083265	0.041591
128	0.447325	0.414727	0.333304	0.249987	0.166653	0.083316	0.041648
256	0.450090	0.415567	0.333325	0.249997	0.166663	0.083329	0.041662
512	0.452101	0.416039	0.333331	0.249999	0.166666	0.083332	0.041666
x_p	0.458333	0.416667	0.333333	0.25	0.166667	0.083333	0.041667

3.3. Phenomenological Renormalization—Location of T_c

Given data for κ_N from strips of two different widths, one can locate the critical line by phenomenological or finite-size renormalization[7,40]; namely, by solving the equation

$$N\kappa_N(\beta^*\mathbf{J}_0) = N'\kappa_{N'}(\beta^*\mathbf{J}_0) \tag{3.11}$$

where $\mathbf{J}_0$ is a fixed direction in the parameter space $\mathbf{K}=\beta\mathbf{J}$. From the point of view of the Bethe ansatz, the most natural implementation of (3.11) for the symmetric eight-vertex model involves the variables p and μ with $w=0$. Thus, we estimate p^* $(=0)$ from the solution p_N^* of

$$N\kappa_N(p^*, \mu) = N'\kappa_{N'}(p^*, \mu) \tag{3.12}$$

The resulting estimates for several values of N with $N'=N-4$ are shown in Fig. 6 as a function of μ.

The choice of variables (p, μ) is rather advantageous, since, as we shall discuss further in the next section, they correspond closely to the actual nonlinear scaling fields of the theory and hence minimize correction terms that would normally be expected in any realistic finite lattice calculation. A more realistic test is to revert to the magnetic spin formulation and write (3.12) as

$$N\kappa_N(\beta^*J_1(1, \alpha)) = N'\kappa_{N'}(\beta^*J_1(1, \alpha)) \tag{3.13}$$

where $\alpha=K_2/K_1$ is fixed. This conforms with Nightingale's approach,[20,21,40] although we are using a different gap.

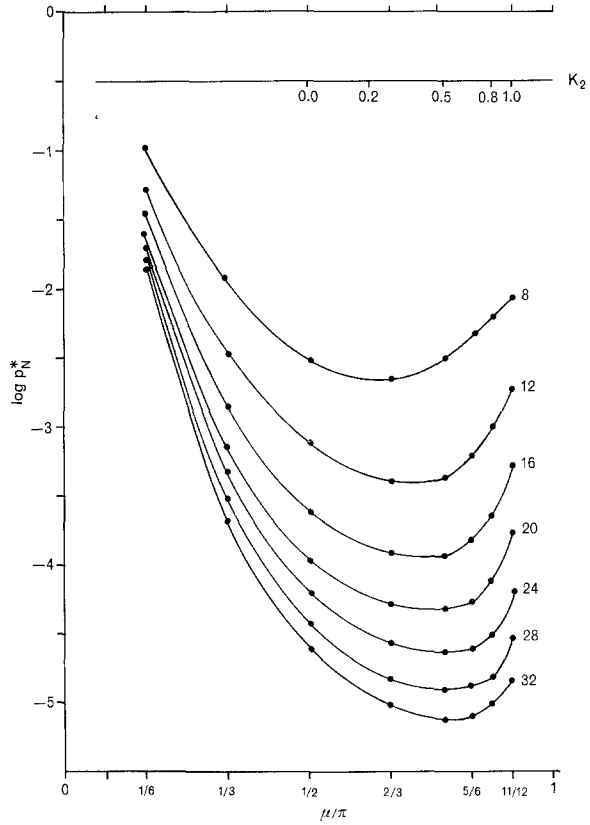

Fig. 6. Finite lattice estimates p_N^* of the bulk critical temperature, $p^* = 0$, with increasing N as a function of the variable μ. Also shown are the corresponding values of the four-spin coupling constant K_2 at criticality.

From the parametrization of the vertex weights given in (2.41) and their relation to the spin couplings in (2.3), the connection between the two formulations can be written as

$$\exp(4K_1) = -\frac{f^2(-(\chi^{-1}\zeta)^{1/2}, p)}{f^2((\chi^{-1}\zeta)^{1/2}, p)} \tag{3.14a}$$

$$\exp(4K_1') = -\frac{f^2(-(\chi\zeta)^{1/2}, p)}{f^2((\chi\zeta)^{1/2}, p)} \tag{3.14b}$$

$$\exp(4K_2) = -\frac{f^2(\chi, p)}{f^2(-\chi, p)} \tag{3.14c}$$

At criticality, these equations reduce to

$$\exp(2K_1) = \cot(\mu/4 - w/4) \tag{3.15a}$$

$$\exp(2K_1') = \cot(\mu/4 + w/4) \tag{3.15b}$$

$$\exp(2K_2) = \tan(\mu/2) \tag{3.15c}$$

Thus, for a given value of K_2 along the critical line, solving (3.13) is equivalent to solving (3.12) at the corresponding value of μ given in (3.15c). The subsequent value of p_N^* then gives the estimate $\beta_N^* J_1$ through Eq. (3.14a). The resulting estimates for the critical line converge rapidly to the exact curve (2.7), in agreement with the earlier studies.[20,21]

3.4. Phenomenological Renormalization—Estimate of ν

Let us now turn to the question of estimating the critical exponent ν from the phenomenological renormalization group. We have[7,22]

$$\left(\frac{d\beta'}{d\beta}\right)^* = r^{1/\nu} = \frac{r(\mathbf{J}_0 \cdot \nabla \kappa_N)^*}{(\mathbf{J}_0 \cdot \nabla \kappa_{N/r})^*} \tag{3.16}$$

where the asterisk indicates that the expressions are to be evaluated at criticality and the gradients are with respect to $\mathbf{K}$. Again choosing $N' = N/r = N - 4$, we obtain the estimators

$$\nu_N^{-1} = 1 + \frac{\ln[(\mathbf{J}_0 \cdot \nabla \kappa_N)^*/(\mathbf{J}_0 \cdot \nabla \kappa_{N-4})^*]}{\ln[N/(N-4)]} \tag{3.17}$$

To extend and clarify the previous finite lattice estimates of ν, we rewrite (3.17) as[40]

$$\nu_N^{-1} = 1 + \frac{\ln[D_1(N)/D_1(N-4)]}{\ln[N/(N-4)]} \tag{3.18}$$

with, in general, derivatives $D_i(m)$ defined by

$$D_i(m) = \left(\frac{\partial \kappa_m}{\partial K_i}\right)^*, \qquad i = 1, 2 \tag{3.19}$$

The exact result for the thermal exponent is[24,4]

$$y_T = \nu^{-1} = \frac{4}{\pi} \tan^{-1}(\exp 2K_2) = \frac{2\mu}{\pi} \tag{3.20}$$

One of the early achievements of phenomenological renormalization was Nightingale's success[20,21] in reproducing this result quantitatively. Now, in order to compare our results with those obtained in the spin formalism, it is necessary to write the derivatives in (3.19) in terms of the more convenient variables (p, μ). The necessary working is straightforward and is outlined in Appendix C. Using results (C3)–(C5) with $w=0$, we have

$$D_1(m)=\frac{1}{2\sin\mu\sin(\mu/2)}\left(\frac{\partial\kappa_m}{\partial p}\right)^*+\frac{2\cos\mu}{\sin(\mu/2)}\left(\frac{\partial\kappa_m}{\partial\mu}\right)^* \tag{3.21a}$$

$$D_2(m)=\frac{1}{4\sin^2(\mu/2)}\left(\frac{\partial\kappa_m}{\partial p}\right)^*+2\cot(\mu/2)\left(\frac{\partial\kappa_m}{\partial\mu}\right)^* \tag{3.21b}$$

3.4.1. Evaluation of Critical Derivatives

Let us briefly consider the evaluation of the derivatives appearing in (3.21). We begin by noting that the derivatives with respect to the variable μ are simply derivatives *along* the critical line, i.e., *marginal* derivatives. It is thus convenient to evaluate these derivatives *numerically* using, for example, the two-sided, four-point formula

$$h'(x)=\frac{h(x-2\Delta x)-8h(x-\Delta x)+8h(x+\Delta x)-h(x+2\Delta x)}{12\Delta x}+O(\Delta x)^4 \tag{3.22}$$

The derivatives with respect to the temperature-like variable p are, however, derivatives *across* the critical line (we shall refer to these as *thermal* derivatives). To use a two-sided derivative as in (3.22), we thus need to be able to calculate $T_0(\zeta)$ and $T_1(\zeta)$ *above* the critical temperature.

Fortunately, in this formalism, the simple interchange $p\leftrightarrow -p$ represents the duality transformation between the low- and high-temperature phases of the model. Consider, first, the largest eigenvalue $T_0(\zeta)$. The Bethe ansatz equations (2.47) involve elliptic functions of nome p^2. As none of the zeros characterizing $T_0(\zeta)$ are explicitly dependent on p, the duality transformation leaves $T_0(\zeta)$ unchanged. We must have

$$(\partial T_0/\partial p)^*=0 \tag{3.23}$$

and so only the derivative of $T_1(\zeta)$ need be considered. Recall that this eigenvalue has an exact zero at $\zeta_1=p$. Duality dictates that $T_1(\zeta)$ maps to an eigenvalue with an exact zero given by $\zeta_1=-p$, the remaining zeros being invariant under the transformation. This is indeed the case; the eigenvalue $T_1(\zeta)$ *crosses* at criticality with the leading eigenvalue in the other sector. We observe that the zero $\zeta_1=-p$ in fact corresponds, in this

language, to a 0-string excitation.[29] Thus, in evaluating the derivative $T_1(\zeta)$ at criticality using (3.22), we also compute the leading 0-string eigenvalue. This eigenvalue has associated quantum numbers $v = v' = v'' = 1$ and in terms of the original variables in Section 2.2 has an exact zero at $z_1 = -q^{1/2}$ (the zero at $z_1 = -1$ is excited to this position). This level gives in fact, in the spin language, the largest eigenvalue with antiperiodic boundary conditions.[6] In Fig. 7 we show these levels schematically as a function of the variable p. We have observed that, in this formalism, quite literally, the *whole* spectrum can be "folded over" the vertical line through $p = 0$.

Alternatively, exact expressions can be derived for the derivatives appearing in (3.21), although such expressions involve solving a further set of linear simultaneous equations for the derivatives of the zeros characterizing $T_0(\zeta)$ and $T_1(\zeta)$. However, for large N in particular, we have chosen to evaluate the derivatives of the mass gap in this manner. This necessitates only the computation of the zeros characterizing $T_0(\zeta)$ and $T_1(\zeta)$ *at* criticality. We derive these equations in Appendix D. Finally, we mention that we have compared our results for the derivatives in (3.21) with the exact "brute force" results for lattice sizes $N = 4$ and $N = 8$. We proceed now to our estimates of the critical exponent ν.

3.4.2. Numerical Results

As an illustrative example of our results, we show in Fig. 8a the finite lattice estimates (3.18) as a function of the four-spin coupling K_2 for the

[6] Using (2.36), (3.1), (3.2), and (3.8) then gives $(5\pi/6 - \mu)\, N^{-2}$ as the leading correction to the free energy per site of the eight-vertex model with antiperiodic boundary conditions in the spin formulation.

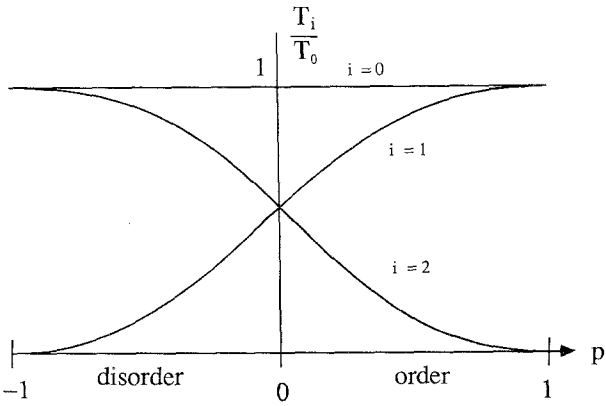

Fig. 7. Schematic illustration of the three leading eigenvalues of the eight-vertex model on a finite lattice. Eigenvalue $T_1(\zeta)$ crosses at criticality with the leading 0-string eigenvalue $T_2(\zeta)$.

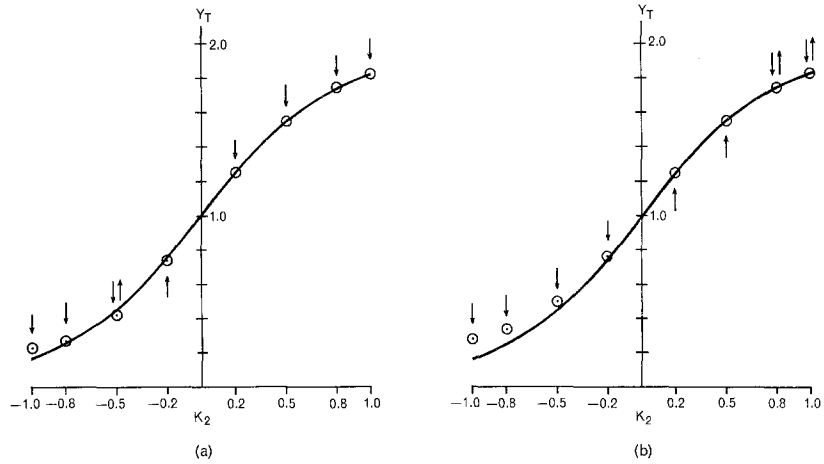

Fig. 8. Estimates of the thermal exponent y_T of the eight-vertex model as a function of the four-spin coupling K_2 obtained from strips of width $N=64$ and $N'=60$. The solid line is the exact value of y_T. The arrows indicate the direction of convergence (see text). (a, b) Results using the mass gaps defined in (3.1) and (3.24), respectively.

particular value $N=64$. Also shown is the direction in which the finite lattice estimates converge to the exact result (3.20); a downward-pointing arrow indicates convergence from above, etc. For the mass gap (3.1), the convergence is *monotonic* for large values of the four-spin coupling. At the particular point $K_2=-0.5$, however, the estimates successively decrease from above the critical temperature until at $N=60$ they begin to converge uniformly from below (the exact value lies between the $N=12$ and $N=16$ estimates).

At first glance these results appear somewhat surprising, as the previous results[20–22] for strips of width up to $N=16$ showed non-monotonic convergence for $K_2 \geqslant 0.5$. Recall, however, that we are using a different gap. We can readily define a further gap by

$$\kappa_N^{(2)} = \ln(T_0/T_2) \tag{3.24}$$

with T_2 the leading eigenvalue in the sector with $v=v'=1$ (as discussed above). The critical derivatives of this gap are easily obtained from those of κ; the derivative with respect to μ is the same, but the thermal derivative has opposite sign (recall Fig. 7).

The finite lattice estimates (3.18) using the gap (3.24) are shown in Fig. 8b, also for $N=64$. Again the convergence is monotonic, with now the estimates at $K_2=0.8$ and $K_2=1.0$ the exceptions. As for the previous gap, such estimates initially approach the bulk critical line from above, but

"overshoot" the exact values. Here this occurs at $N=20$ for $K_2=0.8$ and $N=48$ for $K_2=1.0$. The trend in convergence changes direction at, respectively, $N=32$ and $N=72$.

The common factor in Fig. 8 is the poor convergence for $K_2 \leqslant -0.5$. In the next section, we will relate this to the change [recall (3.8)] found in the convergence rate of estimators of c and the mass gap amplitude in Sections 3.1 and 3.2. (In spin language, the value $\mu=\pi/3$ corresponds to $K_2=-0.274\ldots$.) As we have seen, however, the convergence rate can also be "distorted" by the behavior of the derivatives in (3.21). In particular, for the mass gap (3.24) in which the thermal derivative is negative, the initial overshooting of the exact critical temperatures for large K_2 is reminiscent of the nonmonotonic behavior seen by Nightingale[20,21] and Barber.[22]

Unfortunately, the direct extension of Nightingale's results, by using the same gap, is beyond the scope of this paper. The recovery of this gap from the arrow formulation of the eight-vertex model appears to require imposing *antiperiodic* boundary conditions on the arrows, as has recently been pointed out by Davies.[41]

3.5. Convergence Rates

In Section 3.2, we found that *at* criticality

$$N\kappa_N = 2\pi x_p + O(N^{-\lambda}) \tag{3.25}$$

where λ is given by (3.8). On the basis of conformal invariance, Cardy[34] has shown that the correction terms in (3.25) arise since the physical critical Hamiltonian differs from the conformally invariant fixed-point Hamiltonian by terms involving irrelevant operators.[7]

Writing

$$H_c = H^* + \sum_i \alpha_i O_i \tag{3.26}$$

Cardy showed that a gap, such as κ_N, should behave at criticality as

$$\kappa_N \sim \frac{2\pi}{N}\left(x_p + \sum_i \alpha_i C_{ppi}\left(\frac{2\pi}{N}\right)^{2-x_i} + \cdots\right) \tag{3.27}$$

where x_i (>2) is the anomalous dimension of the operator O_i and C_{ppi} is the relevant (universal) operator algebra coefficient.

[7] The role of irrelevant operators in the corrections to finite-size scaling was pointed out by Barber[7] and discussed in detail by Privman and Fisher[33] (see also Reinicke[42]).

A naive interpretation of our conclusion (3.25) would identify $\lambda+2$ with the dimension of the dominant irrelevant operator (the so-called correction-to-scaling exponent). In the XXZ chain, this identification is, however, incorrect, since the spectrum contains no gaps that can be related to the existence of an operator with such a dimension.[18] While we have not made a similar exhaustive search of the eigenspectrum of the eight-vertex model transfer matrix, the close similarity of the two problems at criticality suggests that the corrections to scaling should be of the same origin. In the XXZ model, these can be explained[7,18] by assuming that two irrelevant operators are involved: O_{I} with dimensions $x_{\mathrm{I}}=4$ and O_{II} with dimension $x_{\mathrm{II}}=1/x_p=2\pi/(\pi-\mu)$. The operator O_{I} belongs to the conformal block of the identity operator and gives rise to "analytic" corrections. On the other hand, O_{II} leads to nonanalytic corrections, but only couples to the relevant operators in *second* order, i.e., $C_{pp\mathrm{II}}=0$. As a result,

$$N\kappa_N \approx 2\pi x_p + A_{\mathrm{I}} N^{-2} + A_{\mathrm{II}} N^{2x_{\mathrm{II}}-4} \tag{3.28}$$

If we accept that this assumption is also valid for the eight-vertex model, we are able to account, not only for the convergence of κ_N and c_N, but also for the convergence of the phenomenological renormalization estimators p_N^* and v_N^*. To do so, we assume that $\kappa_N(p,\mu)$ has the generalized finite-size scaling form

$$\kappa_N(p,\mu) \sim N^{-1} Q(g_T N^{y_T}, g_m, g_{\mathrm{I}} N^{-2}, g_{\mathrm{II}} N^{-y}) \tag{3.29}$$

where $g_T \sim p \sim T - T_c$ is the thermal field, $g_m \sim K_2 \sim \mu - \pi/2$ is marginal, and we have set $y = x_{\mathrm{II}} - 2 = 2\mu/(\pi-\mu)$. To recover (3.28), we require

$$Q(0, g, u, v) = 2\pi x_p + A_{\mathrm{I}}(g)u + A_{\mathrm{II}}(g)v^2 + \cdots \tag{3.30}$$

as $u, v \to 0$. Prediction of the asymptotic behavior of p_N^* and v_N^* requires also the behavior of $Q(x,...)$ for small x. Since this limit involves a relevant variable, it appears, at first sight, that conformal invariance can no longer be used to determine the leading behavior. However, (3.27) remains, in fact, valid for relevant perturbations.[8]

[8] This has also been realized recently by Reinicke,[43] who showed that it was possible, given the knowledge of certain correlation functions, to compute explicitly the coefficients of the scaling function at small argument. It would be interesting to extend Reinicke's calculations to the eight-vertex model.

Hence, we find that

$$Q(x, g, u, v) = 2\pi x_p + A_0(g)\, x[1 + b_1(g)u + b_{II}(g)\, v^2 + \cdots] + A_I(g)u + A_{II}(g)\, v^2 + \cdots \tag{3.31}$$

as $x, u, v \to 0$, where the absence of a term of order xv is due to the same selection rule that prevented a term of order v in (3.30).

With this result, it is straightforward to extend the analysis of Privman and Fisher[33] (see also Barber[22]) to show that

$$p_N^* \sim DN^{-y_T - \lambda}, \qquad N \to \infty \tag{3.32}$$

while

$$v_N^{-1*} \sim v^{-1} + D'N^{-y_T}, \qquad N \to \infty \tag{3.33}$$

The occurrence of logarithmic factors at $\mu = \pi/3$ can also be understood. At this value, $y_I = 2 - x_I$ and $y_{II} = 2 - x_{II}$ satisfy a linear relation, namely $y_I = 2y_{II}$, which results in additional logarithmic factors.[44]

We now turn to the numerical confirmation of the results (3.32) and (3.33). From (3.32), we assume

$$p_N^* \sim DN^{-\omega}, \qquad N \to \infty \tag{3.34}$$

and define estimators

$$\omega_N = \frac{\ln(p_{N-4}^*/p_N^*)}{\ln[N/(N-4)]} \to \omega \qquad \text{as} \quad N \to \infty \tag{3.35}$$

Figure 9 shows this sequence for $N = 16$, 32, and 64. Also shown is the value $\omega = y_T + \lambda$, with the exponent λ defined in (3.8). Unfortunately, the sequence (3.35) cannot in general be calculated for larger N, as p_N^* rapidly approaches the numerical precision of our solutions. Nevertheless, the results shown clearly point to the validity of (3.32).

To test (3.33), we set $y = v^{-1}$, assume

$$y_N^* \sim y + D'N^{-\theta}, \qquad N \to \infty \tag{3.36}$$

and define the estimators

$$\theta_m = \frac{\ln(\Delta y_{2^m}^*/\Delta y_{2^{m+1}}^*)}{\ln 2} \to \theta \qquad \text{as} \quad N \to \infty \tag{3.37}$$

where $\Delta y_N^* = y_N^* - y$. Figure 10 shows this sequence as a function of K_2 for the particular values $m = 4$, 6, and 8. For $K_2 > 0$ and $K_2 < 0$ we have used,

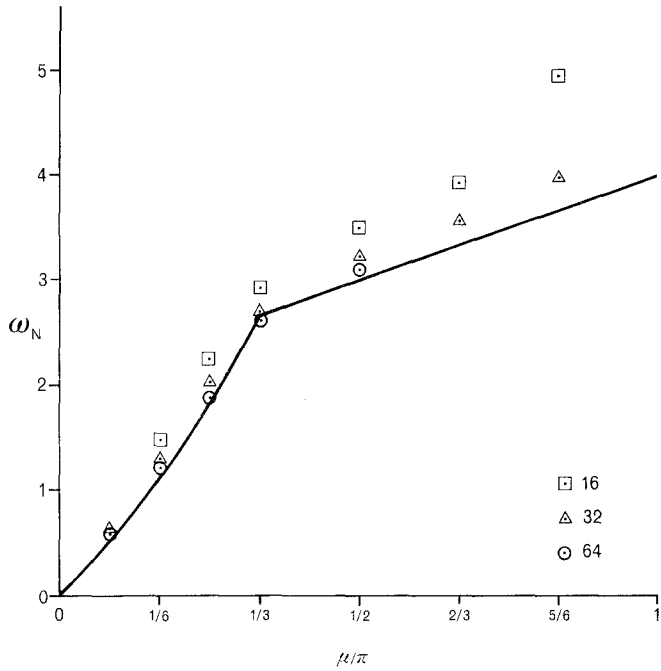

Fig. 9. Estimates ω_N [Eq. (3.35)] of the leading correction to the finite lattice estimates of the critical temperature as a function of μ. The solid line is the exact value $y_T + \lambda$.

respectively, the mass gaps (3.1) and (3.24). The estimators in (3.37) are amenable to extrapolation[7] and in all cases we find excellent agreement with the predictions in (3.33).

The result (3.33) can be reproduced exactly in the Ising limit. Using the results of Appendix D, we find that the derivatives of the mass gaps (3.1) and (3.24) assume the simple form

$$\left(\frac{\partial \kappa}{\partial K_1}\right)^* = -2\sqrt{2}, \qquad \left(\frac{\partial \kappa}{\partial K_2}\right)^* = -2\left(1+\frac{1}{N}\right) \tag{3.38}$$

$$\left(\frac{\partial \kappa^{(2)}}{\partial K_1}\right)^* = 2\sqrt{2}, \qquad \left(\frac{\partial \kappa^{(2)}}{\partial K_2}\right)^* = 2\left(1-\frac{1}{N}\right) \tag{3.39}$$

Thus, for both gaps, the estimators (3.18) yield the exact thermal exponent for all N. However, the corresponding estimators with K_2 derivatives are seen to converge as N^{-1}, in agreement with (3.33).

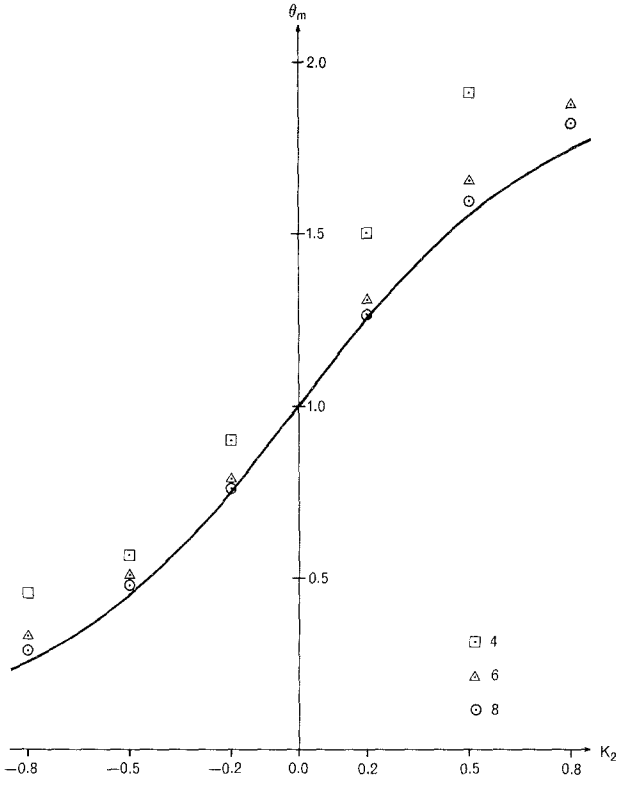

Fig. 10. Estimates θ_m, (3.37), of the leading correction to the finite lattice estimates of the thermal exponent as a function of the four-spin coupling K_2. The solid line is the exact value of y_T given by (3.23).

3.6. Scaling Function

Finally, it is of interest to compute numerically the scaling function for κ. Neglecting corrections due to the irrelevant fields, (3.29) implies that

$$\kappa_N(p, \mu) \sim N^{-1} Q(pN^{1/\nu}; \mu) \tag{3.40}$$

as $N \to \infty$ and $p \to 0$ with $pN^{1/\nu}$ of order unity. Hence, for fixed μ, a plot of $N\kappa_N$ versus $pN^{1/\nu}$ should reduce to a single curve. In Fig. 11 we show such a plot for the particular values $\mu = \pi/3$ and $\mu = 2\pi/3$. We show only the curve obtained from a strip of width $N = 128$; the error is expected to be no greater than the width of each line.

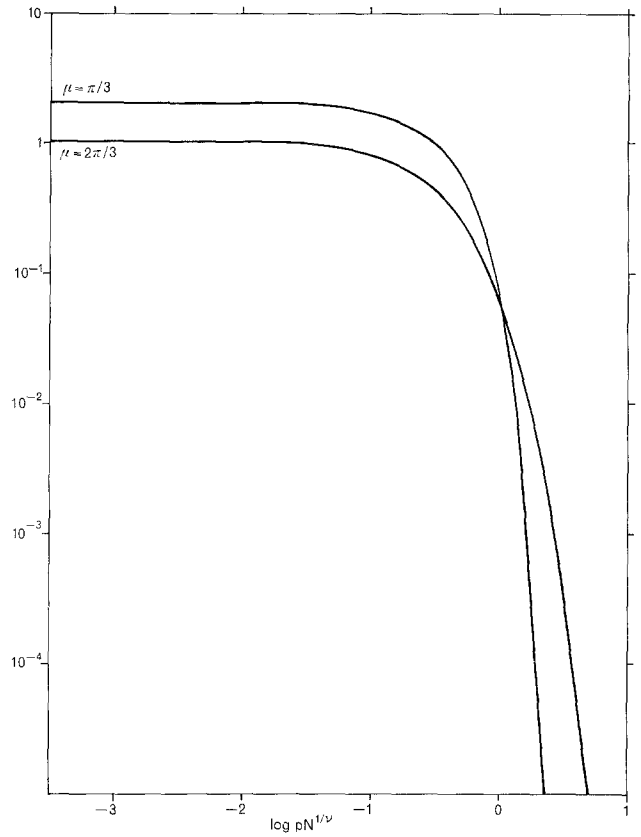

Fig. 11. Scaling function $Q(pN^{1/\nu}; \mu)$ for the eight-vertex model mass gap κ at the particular values $\mu = \pi/3$ and $\mu = 2\pi/3$.

Two asymptotic regimes of the scaling function (3.40) are known. From (3.30) we observe that

$$Q(x; \mu) = \pi - \mu + O(x), \qquad x \to 0 \tag{3.41}$$

while to recover the bulk behavior we require, as usual in finite-size scaling, that

$$Q(x; \mu) = Q_\infty x^{-\nu}, \qquad x \to \infty \tag{3.42}$$

Figure 11 clearly demonstrates the crossover between these two asymptotic regimes.

4. LINEAR SCALING FIELDS

It is very apparent from the discussion in Section 3.5 that criticality in the eight-vertex model involves several scaling fields. On the other hand, conventional phenomenological renormalization, unlike a microscopic renormalization group, gives no direct information on the scaling field structure of a model. Two methods of estimating linear scaling fields and their critical exponents from finite-lattice data have been recently proposed by Barber.[22,23] To formulate these methods, recall[45,46] that for a system described by a set $\mathbf{K}$ of coupling constants the critical exponents and related linear scaling fields are associated with the fixed points $\mathbf{K}^*$ of some microscopic renormalization of the couplings

$$\mathbf{K} \to \mathbf{K}' = \mathscr{R}_r(\mathbf{K}) \tag{4.1}$$

in which r (>1) is the spatial rescaling factor in the transformation. By linearizing (4.1) around a particular fixed point, we obtain the exponents from the eigenvalues $\Lambda_\alpha = r^{y_\alpha}$, $y_\alpha = 2 - x_\alpha$, of the matrix

$$T_{i,j} = \left(\frac{\partial K_i'}{\partial K_j}\right)^* \tag{4.2}$$

where the derivative is evaluated at $\mathbf{K} = \mathbf{K}^*$. The associated linear scaling fields are given by

$$u_\alpha = \mathbf{f}_\alpha \cdot (\mathbf{K} - \mathbf{K}^*) \tag{4.3}$$

where $\mathbf{f}_\alpha$ is the left eigenvector of $\mathbf{T}$ with eigenvalue Λ_α.

4.1. Linear Scaling Fields for the Eight-Vertex Model—Exact Results

Exact expressions for the linear scaling fields of the eight-vertex model in the spin formulation (4.3) can be extracted from (3.14a)–(3.14c) by considering the quantities

$$u_p \approx (\nabla p)^* \cdot (\mathbf{K} - \mathbf{K}^*) \tag{4.4a}$$

$$u_\mu \approx (\nabla \mu)^* \cdot (\mathbf{K} - \mathbf{K}^*) \tag{4.4b}$$

$$u_w \approx (\nabla w)^* \cdot (\mathbf{K} - \mathbf{K}^*) \tag{4.4c}$$

where the derivatives are with respect to $\mathbf{K}$ and are evaluated at criticality. As remarked previously, the variables (p, μ, w) correspond closely to the actual nonlinear scaling fields of the theory [see, e.g., the expression for the

bulk free energy in Eq. (10.12.12) of Ref. 4]. The derivatives in (4.4) are given in Appendix C. Normalizing the fields so that

$$u_1 = (K_1 - K_1^*) + a(1, 1')(K_1' - K_1'^*) + a(1, 2)(K_2 - K_2^*) \tag{4.5a}$$

$$u_1' = (K_1' - K_1'^*) + a(1', 1)(K_1 - K_1^*) + a(1', 2)(K_2 - K_2^*) \tag{4.5b}$$

$$u_2 = (K_2 - K_2^*) + a(2, 1)(K_1 - K_1^*) + a(2, 1')(K_1' - K_1'^*) \tag{4.5c}$$

we obtain

$$a(1, 1') = \frac{\sin(\mu/2 + w/2)}{\sin(\mu/2 - w/2)}, \qquad a(1, 2) = \frac{\sin \mu}{\sin(\mu/2 - w/2)} \tag{4.6a}$$

$$a(1', 1) = -\frac{\sin(\mu/2 - w/2)}{\sin(\mu/2 + w/2)} \tag{4.6a}$$

$$a(1', 2) = \frac{\sin 2\mu \sin w}{\sin(\mu/2 + w/2)[\sin 2\mu - 2\sin(\mu - w)]} \tag{4.6a}$$

$$a(2, 1) = \frac{\cos \mu \sin(\mu/2 - w/2)}{\sin \mu \cos w}, \qquad a(2, 1') = \frac{\cos \mu \sin(\mu/2 + w/2)}{\sin \mu \cos w} \tag{4.6c}$$

These results simplify considerably in two special limits.

4.1.1. Anisotropic Ising Limit $\mu = \pi/2$

In this limit the variable w varies the strength of the anisotropic nearest neighbor couplings on the two independent sublattices. The linear scaling fields (4.5a)–(4.5c) reduce to

$$u_1 = (K_1 - K_1^*) + \frac{\cos w/2 + \sin w/2}{\cos w/2 - \sin w/2}(K_1' - K_1'^*) \tag{4.7a}$$

$$u_1' = (K_1' - K_1'^*) - \frac{\cos w/2 - \sin w/2}{\cos w/2 + \sin w/2}(K_1 - K_1^*) \tag{4.7b}$$

$$u_2 = 0 \tag{4.7c}$$

Recalling (3.15a) and (3.15b), we can write the amplitudes as $a_1 = \sinh 2K_1$ and $a_1' = -1/a_1$, agreeing with the results derived by Barber.[22] The corresponding exponents are $y_1 = 1$ and $y_1' = 0$.

4.1.2. Isotropic Eight-Vertex Limit $w = 0$

Here the variable μ alters the strength of the spin coupling constants through (3.15a) and (3.15c). The linear scaling fields are

$$u_1 = 2(K_1 - K_1^*) + 2\cos(\mu/2)(K_2 - K_2^*) \tag{4.8a}$$

$$u_1' = 0 \tag{4.8b}$$

$$u_2 = (K_2 - K_2^*) + \frac{\cos\mu}{\cos(\mu/2)}(K_1 - K_1^*) \tag{4.8c}$$

Renormalizing as in Barber,[22] we define amplitudes $a_1 = \cos(\mu/2)$ and $a_2 = \cos\mu/\cos(\mu/2)$, which in terms of the four-spin coupling constant K_2 can be written as

$$a_1 = 1/(1+e^{4K_2})^{1/2}, \qquad a_2 = (1-e^{4K_2})/(1+e^{4K_2})^{1/2} \tag{4.9}$$

The amplitude a_1 of the thermal field agrees with Barber's result,[9] while the amplitude a_2 of the subdominant (marginal) field was previously unknown. In this case $y_1 = y_T$ with y_T given in (3.20) and, as for the anisotropic Ising model,[22] $y_2 = 0$.

4.2. Numerical Results

Here we implement and fully test Barber's method A.[22] Using finite-lattice data, this method explicitly constructs the transformation matrix defined in (4.2), from which the scaling fields and exponents readily follow. Specifically, in the isotropic limit, we define 2×2 matrices $\mathbf{L}$ and $\mathbf{M}$ by

$$L_{i,j} = D_j(l_i), \qquad M_{i,j} = D_j(m_i) \tag{4.10}$$

The matrix $\mathbf{T}$ can then be written as[22,23]

$$\mathbf{T} = r\mathbf{M}^{-1}\mathbf{L} \tag{4.11}$$

where the two pairs of strips (l_1, m_1) and (l_2, m_2) are such that $l_i = rm_i$. The linear scaling fields defined in (4.3) can then be found from the right eigenvectors of $\mathbf{T}$,

$$\mathbf{e}_i = (\cos\theta_i, \sin\theta_i), \qquad i = 1, 2 \tag{4.12}$$

with the result that $a_1 = -\cot\theta_2$ and $a_2 = -\tan\theta_1$. As indicated above, the related exponents follow from the eigenvalues through $\Lambda_i = r^{y_i}$, $i = 1, 2$.

In Table V we show sequences of finite lattice estimates obtained from the mass gaps (3.1) and (3.24) at $K_2 = 0.2$, 0.5, 0.8, and 1.0. [Here quantities obtained from (3.1) and (3.24) are denoted by, respectively, (1) and (2).] For convenience we have used triplets of lattice sizes. For a given

[9] A minus sign is missing from the result quoted in Ref. 22.

Table V. Phenomenological Renormalization Estimates of the Exponents $y_1 = y_T$ and $y_2 = y_m$ and Linear Scaling Field Amplitudes $a_1 = a_T$ and $a_2 = a_m$ of the Eight-Vertex Model

r	Lattices	y_1	$a_1^{(1)}$	$a_1^{(2)}$	y_2	$a_2^{(1)}$	$a_2^{(2)}$
$K_4 = 0.2$							
2	(4, 8, 16)	1.242628	0.588362	0.555239	−0.055390	−1.088	−0.377
	(8, 16, 32)	1.246684	0.556942	0.556656	−0.011898	−0.914	−0.487
	(16, 32, 64)	1.247755	0.556814	0.556785	−0.002875	−0.816	−0.562
	(32, 64, 128)	1.248026	0.556801	0.556798	−0.000713	−0.760	−0.609
	(64, 128, 256)	1.248094	0.556799	0.556799	−0.000178	−0.728	−0.638
	(128, 256, 512)	1.248111	0.556799	0.556799	−0.000044	−0.709	−0.656
4/3	(288, 384, 512)	1.248115	0.556799	0.556799	−0.000016	−0.701	−0.664
8/7	(392, 488, 512)	1.248115	0.556799	0.556799	−0.000016	−0.698	−0.667
	Exact	1.248117	0.556799		0	−0.682	
$K_4 = 0.5$							
2	(4, 8, 16)	1.534152	0.347120	0.343404	−0.176223	−10.83	−0.237
	(8, 16, 32)	1.547583	0.345415	0.345101	−0.037280	−5.703	−0.731
	(16, 32, 64)	1.550483	0.345263	0.345252	−0.004215	−4.044	−1.138
	(32, 64, 128)	1.551003	0.345258	0.345257	−0.000904	−3.405	−1.390
	(64, 128, 256)	1.551126	0.345258	0.345258	−0.000218	−3.028	−1.584
	(128, 256, 512)	1.551156	0.345258	0.345258	−0.000054	−2.783	−1.735
4/3	(288, 384, 512)	1.551162	0.345258	0.345258	−0.000019	−2.652	−1.826
8/7	(392, 488, 512)	1.551163	0.345258	0.345258	−0.000014	−2.616	−1.853
	Exact	1.551166	0.345258		0	−2.206	
$K_4 = 0.8$							
2	(4, 8, 16)	1.744949	0.195969	0.199856	0.139950	23.77	1.198
	(8, 16, 32)	1.730084	0.198175	0.197632	−0.182414	17.92	1.528
	(16, 32, 64)	1.744552	0.197917	0.197890	−0.025515	−83.54	−0.084
	(32, 64, 128)	1.746145	0.197903	0.197903	−0.001312	−17.49	−1.135
	(64, 128, 256)	1.746302	0.197903	0.197903	−0.000241	−13.02	−1.586
	(128, 256, 512)	1.746336	0.197903	0.197903	−0.000056	−10.75	−1.956
4/3	(288, 384, 512)	1.746342	0.197903	0.197903	−0.000020	−9.587	−2.211
8/7	(392, 488, 512)	1.746344	0.197903	0.197903	−0.000014	−9.271	−2.291
	Exact	1.746347	0.197903		0	−4.657	
$K_4 = 1.0$							
2	(4, 8, 16)	1.944347	0.130026	0.138325	0.579105	27.96	2.061
	(8, 16, 32)	1.806340	0.134140	0.134085	−0.114101	12.80	4.368
	(16, 32, 64)	1.820475	0.134146	0.134080	−0.119200	15.18	3.699
	(32, 64, 128)	1.828338	0.134113	0.134112	−0.005446	129.6	0.548
	(64, 128, 256)	1.828677	0.134113	0.134112	−0.000305	−88.90	−0.468
	(128, 256, 512)	1.828715	0.134113	0.134112	−0.000060	−48.51	−0.968
4/3	(288, 384, 512)	1.828722	0.134113	0.134112	−0.000020	−37.14	−1.304
8/7	(392, 488, 512)	1.828723	0.134113	0.134112	−0.000014	−34.55	−1.412
	Exact	1.828726	0.134113		0	−7.188	

triplet, a different matrix **T** is constructed from each gap, yet both matrices are seen to have common eigenvalues and thus produce the same exponent estimates.

As was borne out in the earlier results,[22] the agreement of the thermal field and its exponent with the exact values is excellent for all K_2. Further, we observe that for $K_2 \geqslant 0.5$ the initial estimates in the sequence for y_1 are nonmonotonic. As we saw in Section 3, however, the sequences settle down into monotonic behavior as they enter into the asymptotic regime. For the triplet of largest lattice sizes the exponent estimates are of similar accuracy for all of the K_2 values shown. In agreement with the earlier results, the estimates of the amplitude of the subdominant (marginal) scaling field and its exponent are poor for the lattice sizes normally available to direct diagonalization. Unfortunately, the amplitude of the marginal field is *still* poorly determined for large values of K_2, even for the *largest* lattice sizes.

Finally, we consider a general triplet of lattice sizes (N, rN, r^2N) in the Ising limit. Using the exact results (3.38) and (3.39) to construct the matrices defined in (4.10), we find both gaps give

$$\mathbf{T} = \begin{bmatrix} r & (r-1)/\sqrt{2} \\ 0 & 1 \end{bmatrix} \tag{4.13}$$

independent of N. Thus, in the isotropic Ising limit, we construct the *exact* transformation matrix, from which we obtain the exact exponents and scaling field amplitudes: $y_1 = 1$, $y_2 = 0$, $a_1 = 1/\sqrt{2}$, and $a_2 = 0$.

5. SUMMARY AND CONCLUSION

In this paper we have reformulated and numerically solved the Bethe ansatz equations for the eight-vertex model on a finite lattice. An approximation scheme, increasing in accuracy with system size, has been used to provide accurate starting points in the numerical solution of the finite system of equations. By using this method, we obtained the three largest eigenvalues, and subsequently two mass gaps, on infinitely long strips of width up to 512 sites.

Our discussion in Section 3 of the convergence of finite lattice estimates with increasing system size has helped to clarify the anomalous behavior seen in earlier studies. We find that the free energy per site approaches its bulk limit as

$$f_N = f_\infty - \tfrac{1}{6}\pi N^{-2} + O(N^{-2-\lambda}) \tag{5.1}$$

while the mass gap (3.1) behaves as

$$N\kappa_N = 2\pi x_p + O(N^{-\lambda}) \tag{5.2}$$

with x_p the scaling dimension (3.10) of the polarization operator.

The correction exponent λ is

$$\lambda = \min(2, 4\mu/(\pi - \mu)) \tag{5.3}$$

This behavior is the same as found in the XXZ chain.[17,18,10,11] Finite lattice estimates of the critical temperature ($p = 0$) converge as

$$p_N^* = O(N^{-y_T - \lambda}) \tag{5.4}$$

here $y_T = 1/\nu$ is the thermal exponent (3.20). On the other hand, estimates of the exponent ν obtained from phenomenological renormalization converge as

$$\nu_N^* = \nu + O(N^{-y_T}) \tag{5.5}$$

The corrections in (5.1), (5.2), (5.4), and (5.5) account for the deterioration in convergence seen[20 22,35,39] when the four-spin coupling K_2 is in the range $K_2 < -0.3$. On the other hand, for large positive values of the four-spin coupling, the above results predict that the convergence should be more rapid than for small values of K_2. The poor convergence seen for the lattice sizes ($N \sim 16$) normally available to direct diagonalization can be attributed to relatively large amplitudes in the correction terms, and also for the estimates of ν, to the behavior of the derivatives, particularly sign changes, that appear in the finite lattice estimators.

In Section 4 we have derived exact expressions for the amplitudes of the linear scaling fields and compared the results with a recently proposed method[22,23] of estimating linear scaling fields from finite lattice data. This involved the explicit (phenomenological) construction of the transformation matrix (4.2) appearing in the renormalization group formalism. Apart from the large K_2 estimates of the subdominant (marginal) scaling field, which becomes large in magnitude, the results obtained were in excellent agreement with the exact values.

Our calculations can be extended in several directions. The observed slow convergence for the interfacial tension defined by (2.37) should be obviated by using a definition incorporating a sum over the relevant *band* of eigenvalues. Also, we mention that the calculations presented in this paper can be repeated in the *full* parameter space of the model. This would

allow a further test of the methods proposed for extracting linear scaling fields and an investigation of the effect of anisotropy on finite-size scaling and its corrections in the eight-vertex model.

APPENDIX A

Three useful identities involving the elliptic function $f(z, q)$ defined in (2.1) are

$$f(z^{-1}, q) = -z^{-1} f(z, q) \tag{A1}$$

$$f(qz^{-1}, q^2) = f(qz, q^2) \tag{A2}$$

$$\frac{f(z, q) f(z, -q)}{f(w, q) f(w, -q)} = \frac{f(z^2, q^2)}{f(w^2, q^2)} \tag{A3}$$

APPENDIX B. CONJUGATE MODULUS TRANSFORMATIONS

To find a conjugate modulus identify for the elliptic function $f(z, q)$ we need the standard (apart from an irrelevant factor) elliptic theta function[4,32]

$$\theta(u, q) = \sin u \prod_{m=1}^{\infty} (1 - 2q^m \cos 2u + q^{2m})(1 - q^m) = \tfrac{1}{2} i e^{-iu} f(e^{2iu}, q) \tag{B1}$$

This function is also related to $f(z, q)$ by the conjugate modulus identify[4]

$$\theta(u, e^{-\varepsilon}) = -\frac{1}{2}\left(\frac{2\pi}{\varepsilon}\right)^{1/2} \exp\left[\frac{\varepsilon}{8} - \frac{\pi^2}{2\varepsilon} - \frac{2u(\pi + u)}{\varepsilon}\right] f(e^{4\pi u/\varepsilon}, e^{-4\pi^2/\varepsilon}) \tag{B2}$$

Comparison of (B1) and (B2) results in

$$f(e^{2iu}, e^{-\varepsilon}) = i\left(\frac{2\pi}{\varepsilon}\right)^{1/2} \exp\left[iu + \frac{\varepsilon}{8} - \frac{\pi^2}{2\varepsilon} - \frac{2u(\pi + u)}{\varepsilon}\right] f(e^{4\pi u/\varepsilon}, e^{-4\pi^2/\varepsilon}) \tag{B3}$$

Since the parametrization of the weights (2.4) and the functional relations (2.9) involve only ratios of elliptic functions, we may use (B3) to define transformation rules:

$$f(e^{i\pi u/I}, q^2) \sim \exp\left(\frac{i\pi u}{2I} - \frac{\pi u}{2I'} - \frac{\pi u^2}{4II'}\right) f(e^{\pi u/I}, p) \tag{B4}$$

$$f(e^{i\pi u/I}, q) \sim \exp\left(\frac{i\pi u}{2I} - \frac{\pi u}{I'} - \frac{\pi u^2}{2II'}\right) f(e^{2\pi u/I'}, p^2) \tag{B5}$$

APPENDIX C

In this appendix we give the details in the derivation of the derivatives of the variables (p, μ, w) with respect to the spin coupling constants $\mathbf{K} = (K_1, K_1', K_2)$. The connection between the sets of variables is given in Eqs. (3.14a)–(3.14c). Recalling the definition (2.1) of the elliptic function $f(z, q)$, we have, to first order in p,

$$\begin{aligned} \exp(2K_1) &= \cot(\mu/4 - w/4)[1 + 4p\cos(\mu/2 - w/2)] \\ \exp(2K_1') &= \cot(\mu/4 + w/4)[1 + 4p\cos(\mu/2 + w/2)] \\ \exp(2K_2) &= \tan(\mu/2)(1 - 4p\cos\mu) \end{aligned} \tag{C1}$$

By differentiating these equations, first with respect to K_1, we obtain

$$\begin{aligned} \left(\frac{\partial\mu}{\partial K_1}\right)^* &= 4\sin\mu\cos\mu\left(\frac{\partial p}{\partial K_1}\right)^* \\ 0 &= \sin(\mu + w)\left(\frac{\partial p}{\partial K_1}\right)^* - \frac{1}{4}\left[\left(\frac{\partial\mu}{\partial K_1}\right)^* + \left(\frac{\partial w}{\partial K_1}\right)^*\right] \\ \sin\left(\frac{\mu}{2} - \frac{w}{2}\right) &= \sin(\mu - w)\left(\frac{\partial p}{\partial K_1}\right)^* - \frac{1}{4}\left[\left(\frac{\partial\mu}{\partial K_1}\right)^* - \left(\frac{\partial w}{\partial K_1}\right)^*\right] \end{aligned} \tag{C2}$$

Now (C2) simply represents a system of three equations in three unknowns, from which we can readily solve for the derivatives:

$$\left(\frac{\partial p}{\partial K_1}\right)^* = \frac{\sin(\mu/2 - w/2)}{2\sin\mu(\cos w - \cos\mu)} \tag{C3a}$$

$$\left(\frac{\partial\mu}{\partial K_1}\right)^* = \frac{2\cos\mu\sin(\mu/2 - w/2)}{\cos w - \cos\mu} \tag{C3b}$$

$$\left(\frac{\partial w}{\partial K_1}\right)^* = \frac{2\sin(\mu/2 - w/2)}{\cos w - \cos\mu}\left[\frac{\sin(\mu + w)}{\sin\mu} - \cos\mu\right] \tag{C3c}$$

In a similar manner we obtain the remaining derivatives,

$$\left(\frac{\partial p}{\partial K_1'}\right)^* = \frac{\sin(\mu/2 + w/2)}{2\sin\mu(\cos w - \cos\mu)} \tag{C4a}$$

$$\left(\frac{\partial\mu}{\partial K_1'}\right)^* = \frac{2\cos\mu\sin(\mu/2 + w/2)}{\cos w - \cos\mu} \tag{C4b}$$

$$\left(\frac{\partial w}{\partial K_1'}\right)^* = \frac{2\sin(\mu/2 + w/2)}{\cos w - \cos\mu}\left[\cos\mu - \frac{\sin(\mu - w)}{\sin\mu}\right] \tag{C4c}$$

and

$$\left(\frac{\partial p}{\partial K_2}\right)^* = \frac{1}{2(\cos w - \cos \mu)} \tag{C5a}$$

$$\left(\frac{\partial \mu}{\partial K_2}\right)^* = \frac{2\cos w - \sin \mu}{\cos w - \cos \mu} \tag{C5b}$$

$$\left(\frac{\partial w}{\partial K_2}\right)^* = \frac{2\sin w \cos \mu}{\cos w - \cos \mu} \tag{C5c}$$

APPENDIX D. DERIVATIVES OF THE MASS GAP

In this appendix we derive expressions for the derivative of the mass gap (3.1) with respect to the variables p and μ. These expressions are to be evaluated at criticality. We consider first the derivative with respective to p.

D1. Thermal Derivative

Using (3.23), we have

$$\left(\frac{\partial \kappa}{\partial p}\right)^* = -\left(\frac{1}{T_1}\frac{\partial T_1}{\partial p}\right)^* \tag{D1}$$

It suffices to consider the eigenvalue equation (2.49) in the form

$$T_1(1) = F(\chi)\frac{f(p\chi^2)}{f(p)}\prod_{j=1}^{n-2}\frac{f(\chi^2\zeta_j)}{f(\zeta_j)} \tag{D2}$$

as the neglected prefactors can be seen to make no contribution to the derivative in the limit $p = 0$. In (D2), for ease of notation, we have dropped the explicit functional dependence on nome p^2.

The logarithmic derivative of (D2), and subsequently Eq. (D1), can be written as a sum of three terms, A, B, and C, with

$$A = \frac{1}{f(p\chi^2)}\frac{\partial f(p\chi^2)}{\partial p} - \frac{1}{f(p)}\frac{\partial f(p)}{\partial p} \tag{D3a}$$

$$B = \frac{1}{F(\chi)}\frac{\partial F(\chi)}{\partial p} \tag{D3b}$$

$$C = \sum_{j=1}^{n-2}\left[\frac{1}{f(\chi^2\zeta_j)}\frac{\partial f(\chi^2\zeta_j)}{\partial p} - \frac{1}{f(\zeta_j)}\frac{\partial f(\zeta_j)}{\partial p}\right] \tag{D3c}$$

Given the definitions (2.1), (2.34b), and (2.35) of the functions appearing in (D2), and the knowledge that none of the $n-2$ zeros appearing in the summation for C are explicitly dependent on p, the evaluation of the terms in (D3) in the limit $p=0$ is relatively straightforward; care need only be taken with the exact zero at p appearing in the function $F(\chi)$. The results are

$$A^* = 4\sin^2\mu \tag{D4a}$$

$$B^* = 4\sin 2\mu \frac{B_1}{B_2} \tag{D4b}$$

$$C^* = \sum_{j=1}^{n/2-1} \left[\frac{\zeta_j - \zeta_j^{-1}}{1+\zeta_j^2 - 2\zeta_j \cos 2\mu} + \frac{1}{\zeta_j}\left(\frac{1+\zeta_j}{1-\zeta_j}\right)\right]\left(\frac{\partial \zeta_j}{\partial p}\right)^* \tag{D4c}$$

with

$$B_1 = -1 + \sum_{j=1}^{n/2-1} \frac{\zeta_j^2 - 1}{(1+\zeta_j^2 - 2\zeta_j \cos 2\mu)^2}\left(\frac{\partial \zeta_j}{\partial p}\right)^* \tag{D5a}$$

$$B_2 = \frac{1+2(N-1)\cos^2\mu/2}{\sin\mu} - 4\sin 2\mu \sum_{j=1}^{n/2-1} \frac{\zeta_j}{1+\zeta_j^2 - 2\zeta_j \cos 2\mu} \tag{D5b}$$

Here again we have used the fact that the zeros are in reciprocal pairs, apart from the zero at p and the stationary zero at 1 (recall also that n is even).

A system of equations for the derivatives of the zeros is readily derived from the Bethe ansatz equations (2.47). As remarked in Section 2.4, the zero at p satisfies one of the equations, leaving the system given in (2.58). The stationary zero satisfies one of these equations (again, the key point is that the zeros are in reciprocal pairs) and this system can further be written as

$$\chi^{-4}\left[\frac{f(\chi\zeta_j)}{f(\chi^{-1}\zeta_j)}\right]^N \frac{f(\chi^{-2}\zeta_j)\, f(p\chi^{-2}\zeta_j)}{f(\chi^2\zeta_j)\, f(p\chi^2\zeta_j)} \prod_{\substack{k=1 \\ \neq j}}^{n-2} \frac{f(\chi^{-2}\zeta_j/\zeta_k)}{f(\chi^2\zeta_j/\zeta_k)} = 1, \qquad j = 1,\ldots, n-2 \tag{D6}$$

On taking a logarithmic derivative, each zero must satisfy

$$NE_1 + E_2 + E_3 + E_4 = 0 \tag{D7}$$

where

$$E_1 = \frac{1}{f(\chi\zeta_j)}\frac{\partial f(\chi\zeta_j)}{\partial p} - \frac{1}{f(\chi^{-1}\zeta_j)}\frac{\partial f(\chi^{-1}\zeta_j)}{\partial p} \tag{D8a}$$

$$E_2 = \frac{1}{f(\chi^{-2}\zeta_j)} \frac{\partial f(\chi^{-2}\zeta_j)}{\partial p} - \frac{1}{f(\chi^2\zeta_j)} \frac{\partial f(\chi^2\zeta_j)}{\partial p} \tag{D8b}$$

$$E_3 = \frac{1}{f(p\chi^{-2}\zeta_j)} \frac{\partial f(p\chi^{-2}\zeta_j)}{\partial p} - \frac{1}{f(p\chi^2\zeta_j)} \frac{\partial f(p\chi^2\zeta_j)}{\partial p} \tag{D8c}$$

$$E_4 = \sum_{k=1}^{n-2} \left[\frac{1}{f(\chi^{-2}\zeta_j/\zeta_k)} \frac{\partial f(\chi^{-2}\zeta_j/\zeta_k)}{\partial p} - \frac{1}{f(\chi^2\zeta_j/\zeta_k)} \frac{\partial f(\chi^2\zeta_j/\zeta_k)}{\partial p} \right] \tag{D8d}$$

On defining the quantity

$$u_j = (\partial\zeta_j/\partial p)^* \tag{D9}$$

we find that Eqs. (D8), in the limit $p = 0$, reduce to

$$E_1^* = \frac{-2i(\sin\mu)\, u_j}{1 + \zeta_j^2 - 2\zeta_j \cos\mu} \tag{D10a}$$

$$E_2^* = \frac{2i(\sin 2\mu)\, u_j}{1 + \zeta_j^2 - 2\zeta_j \cos 2\mu} \tag{D10b}$$

$$E_3^* = 2i(\sin 2\mu)(\zeta_j - \zeta_j^{-1}) \tag{D10c}$$

$$E_4^* = 2i \sin 2\mu \sum_{k=1}^{n-2} \frac{\zeta_k u_j - \zeta_j u_k}{\zeta_j^2 + \zeta_k^2 - 2\zeta_j\zeta_k \cos 2\mu} \tag{D10d}$$

Insertion of these results into (D7) leads to a linear, nonhomogeneous system of equations for the u_j. Specifically, this system of equations can be written in the form

$$G_j u_j + \sum_{k=1}^{n/2-1} H_{jk} u_k = 2(\cos\mu)(\zeta_j^{-1} - \zeta_j), \qquad j = 1, \ldots, n-2 \tag{D11}$$

where

$$G_j = G_j^{(1)} + G_j^{(2)} \tag{D12a}$$

$$H_{jk} = 2\zeta_j \cos\mu \left(\frac{1}{1 + \zeta_j^2\zeta_k^2 - 2\zeta_j\zeta_k \cos 2\mu} - \frac{1}{\zeta_j^2 + \zeta_k^2 - 2\zeta_j\zeta_k \cos 2\mu} \right) \tag{D12b}$$

with

$$G_j^{(1)} = \frac{2\cos\mu}{1 + \zeta_j^2 - 2\zeta_j \cos 2\mu} - \frac{N}{1 + \zeta_j^2 - 2\zeta_j \cos\mu} + \frac{4\zeta_j \cos\mu}{1 + \zeta_j^4 - 2\zeta_j^2 \cos 2\mu} \tag{D12c}$$

$$G_j^{(2)} = 2\cos\mu \sum_{k=1}^{n/2-1} \zeta_k \left[\frac{1}{\zeta_j^2 + \zeta_k^2 - 2\zeta_j\zeta_k \cos 2\mu} - \frac{1}{1 + \zeta_j^2\zeta_k^2 - 2\zeta_j\zeta_k \cos 2\mu} \right] \tag{D12d}$$

The system (D11) is invariant under the transformation $\zeta_j \to \zeta_j^{-1}$, so that half of the equations are redundant; we need only consider solving (D11) for u_j with $j = 1,..., n/2 - 1$. Note that all of the u_j vanish in the Ising limit $\mu = \pi/2$ and the only contribution to (D1) is from the term (D4a).

Finally we remark that the above equations can be written in perhaps a more elegant form by setting $\zeta_j = \exp(-2\alpha_j)$. In this case one could alternatively consider the Bethe ansatz equations in the form (2.59). We adopt this approach for the derivatives with respect to μ.

D2. Marginal Derivatives

Here we are actually *at* criticality (we suppress the asterisk notation for convenience). We can consider eigenvalues (2.67) and (2.68) in the form

$$T_0 = \prod_{j=1}^{n/2} \frac{\cosh 2\alpha_j - \cos 2\mu}{\cosh 2\alpha_j - 1} \tag{D13}$$

$$T_1 = E \prod_{j=1}^{n/2-1} \frac{\cosh 2\alpha_j - \cos 2\mu}{\cosh 2\alpha_j - 1} \tag{D14}$$

where the quantity E is defined in (2.69). The logarithmic derivatives are

$$\frac{1}{T_0}\frac{\partial T_0}{\partial \mu} = \sum_{j=1}^{n/2} R_j \tag{D15}$$

$$\frac{1}{T_1}\frac{\partial T_1}{\partial \mu} = \frac{1}{E}\frac{\partial E}{\partial \mu} + \sum_{j=1}^{n/2-1} R_j \tag{D16}$$

where we have set

$$R_j = 2\left[\frac{w_j \sinh 2\alpha_j + \sin 2\mu}{\cosh 2\alpha_j - \cos 2\mu} - \frac{w_j \sinh 2\alpha_j}{\cosh 2\alpha_j - 1}\right] \tag{D17}$$

and defined the derivative w_j by

$$w_j = \partial \alpha_j / \partial \mu \tag{D18}$$

From (2.69) we have

$$\frac{\partial E}{\partial \mu} = (1-N)\sin\mu - \sum_{j=1}^{n/2-1} \frac{4(\sin\mu)(3\cos^2\mu - 1)}{\cosh 2\alpha_j - \cos 2\mu} + \sum_{j=1}^{n/2-1} \frac{4(\sin\mu \sin 2\mu)(w_j \sinh 2\alpha_j + \sin 2\mu)}{(\cosh 2\alpha_j - \cos 2\mu)^2} \tag{D19}$$

To derive equations for the w_j we consider the Bethe ansatz equations (2.58) and (2.59) with $p=0$. In particular, we write these equations as, respectively,

$$N\varphi(\alpha_j, \mu/2) = 2\pi I_j + \sum_{\substack{k=1 \\ k \neq j}}^{n/2} [\varphi(\alpha_j - \alpha_k, \mu) + \varphi(\alpha_j + \alpha_k, \mu)] \qquad (j = 1,..., n/2) \tag{D20}$$

$$N\varphi(\alpha_j, \mu/2) = 2\pi I_j + \varphi(\alpha_j, \mu) + \sum_{\substack{k=1 \\ k \neq j}}^{n/2-1} [\varphi(\alpha_j - \alpha_k, \mu) + \varphi(\alpha_j + \alpha_k, \mu)] \qquad (j = 1,..., n/2 - 1) \tag{D21}$$

We wish to differentiate these equations with respect to μ. From the definition (2.53) of the function $\varphi(\alpha, \mu)$ we have, after some algebra, the intermediate results

$$\frac{\partial \varphi(\alpha, \mu)}{\partial \mu} = \left(\sin 2\mu \frac{\partial \alpha}{\partial \mu} - \sinh 2\alpha \right) \Omega(\alpha, \mu) \tag{D22a}$$

$$\frac{\partial \varphi(\alpha, \mu/2)}{\partial \mu} = \left(\sin \mu \frac{\partial \alpha}{\partial \mu} - \frac{1}{2} \sinh 2\alpha \right) \Omega\left(\alpha, \frac{\mu}{2}\right) \tag{D22b}$$

where we have defined the quantity $\Omega(\alpha, \mu)$ by

$$\Omega(\alpha, \mu) = \frac{1}{\cosh^2 \alpha - \cos^2 \mu} \tag{D23}$$

Given these results, the system of equations associated with the eigenvalue T_0 can be written in the form

$$U_j w_j + \sum_{\substack{k=1 \\ k \neq j}}^{n/2} V_{jk} w_k = W_j, \qquad j = 1,..., n/2 \tag{D24}$$

where

$$U_j = N(\sin \mu)\, \Omega(\alpha_j, \mu/2) - 2(\sin 2\mu)\, \Omega(2\alpha_j, \mu) - (\sin 2\mu) \sum_{\substack{k=1 \\ k \neq j}}^{n/2} [\Omega(\alpha_j - \alpha_k, \mu) + \Omega(\alpha_j + \alpha_k, \mu)] \tag{D25a}$$

$$V_{jk} = (\sin 2\mu)[\Omega(\alpha_j - \alpha_k, \mu) - \Omega(\alpha_j + \alpha_k, \mu)] \tag{D25b}$$

and

$$W_j = \tfrac{1}{2}N(\sinh 2\alpha_j)\,\Omega(\alpha_j, \mu/2) - (\sinh 4\alpha_j)\,\Omega(2\alpha_j, \mu) - \sum_{\substack{k=1 \\ \neq j}}^{n/2} \{[\sinh 2(\alpha_j - \alpha_k)]\,\Omega(\alpha_j - \alpha_k, \mu) + [\sinh 2(\alpha_j + \alpha_k)]\,\Omega(\alpha_j + \alpha_k, \mu)\} \tag{D25c}$$

The equations associated with T_1 are of the same form as (D24), except with $j, k = 1,..., n/2 - 1$. Slight modifications arise, however, from the extra term in (D21). Rather than writing the equations out in full, we mention only that the quantities $-(\sin 2\mu)\,\Omega(\alpha_j, \mu)$ and $-(\sinh 2\alpha_j)\,\Omega(\alpha_j, \mu)$ need to be added to, respectively, Eqs. (D25a) and (D25c).

Finally, we remark that the solution of the systems (D11) and (D24) posed no numerical problems; again we used a standard library package.[47]

ACKNOWLEDGMENTS

It is a pleasure to acknowledge profitable discussions with Prof. R. J. Baxter, Dr. F. C. Alcaraz, Dr. B. Davies, and Dr. C. J. Hamer. One of the authors (M.T.B.) acknowledges support from a Commonwealth Postgraduate Research Award. The work of M.N.B. at the University of California was supported in part by the National Science Foundation through grant PHY82-17853, supplemented by funds from the National Aeronautics and Space Administration.

REFERENCES

1. E. H. Lieb and F. Y. Wu, in *Phase Transitions and Critical Phenomena*, C. Domb and M. S. Green, eds. (Academic Press, London, 1972), Vol. 1, p. 331.
2. H. B. Thacker, *Rev. Mod. Phys.* **53**:253 (1981).
3. M. Fowler, *J. Appl. Phys.* **53**:2048 (1982).
4. R. J. Baxter, *Exactly Solved Models in Statistical Mechanics* (Academic Press, London, 1982).
5. M. Gaudin, *La Fonction d'Onde de Bethe* (Masson, Paris, 1983).
6. A. M. Tsvelick and P. B. Weigmann, *Adv. Phys.* **32**:453 (1983).
7. M. N. Barber, in *Phase Transitions and Critical Phenomena*, C. Domb and J. L. Lebowitz, eds. (Academic Press, London, 1983), Vol. 8, p. 146.
8. H. J. de Vega and F. Woynarovich, *Nucl. Phys. B* **251**:439 (1985).
9. C. J. Hamer, *J. Phys. A* **18**:L1133 (1986).
10. C. J. Hamer, *J. Phys. A* **19**:3335 (1986).
11. F. Woynarovich and H.-P. Eckle, *J. Phys. A* **20**:L97 (1987).
12. H. O. Martin and H. J. de Vega, *Phys. Rev. B* **32**:5959 (1985).

13. C. J. Hamer, *J. Stat. Phys.* **47**:331 (1987).
14. W. Grieger, *Phys. Rev. B* **30**:344 (1984).
15. J. Borysowicz, T. A. Kaplan, and P. Horsch, *Phys. Rev. B* **31**:1590 (1985).
16. L. V. Avdeev and B. D. Dörfel, *J. Phys. A* **19**:L13 (1986).
17. F. C. Alcaraz, M. N. Barber, and M. T. Batchelor, *Phys. Rev. Lett.* **58**:771 (1987).
18. F. C. Alcaraz, M. N. Barber, and M. T. Batchelor, Conformal invariance, the *XXZ* chain, and the operator content of two-dimensional critical systems, preprint.
19. F. C. Alcaraz, M. N. Barber, M. T. Batchelor, R. J. Baxter, and G. R. W. Quispel, Surface exponents of the quantum *XXZ*, Ashkin–Teller, and Potts models, preprint.
20. M. P. Nightingale, *Phys. Lett.* **59A**:486 (1977).
21. M. P. Nightingale, *Proc. K. Ned. Akad. Wet. B* **82**:235 (1979).
22. M. N. Barber, *Physica* **130A**:171 (1985).
23. M. N. Barber, *Phys. Rev. B* **27**:5879 (1983).
24. R. J. Baxter, *Ann. Phys. (N.Y.)* **70**:193 (1972).
25. R. J. Baxter, *Ann. Phys. (N.Y.)* **76**:1, 25, 48 (1973).
26. F. Y. Wu, *Phys. Rev. B* **4**:2312 (1971).
27. L. P. Kadanoff and F. J. Wegner, *Phys. Rev. B* **4**:3989 (1971).
28. R. J. Baxter, *J. Stat. Phys.* **8**:25 (1973).
29. J. D. Johnson, S. Krinsky, and B. M. McCoy, *Phys. Rev. A* **8**:256 (1973).
30. L. A. Takhtadzhan and L. D. Faddeev, *Russ. Math. Surv.* **34**:11 (1979).
31. NAG routine C05NBF, Numerical Algorithms Group.
32. I. S. Gradshteyn and I. M. Ryzhik, *Table of Integrals, Series and Products* (Academic Press, New York, 1980).
33. V. Privman and M. E. Fisher, *J. Phys. A* **16**:L295 (1983).
34. J. L. Cardy, *Nucl. Phys. B* **270[FS16]**:186 (1986).
35. H. W. J. Blöte, J. L. Cardy, and M. P. Nightingale, *Phys. Rev. Lett.* **56**:742 (1986).
36. I. Affleck, *Phys. Rev. Lett.* **56**:746 (1986).
37. D. Friedan, Z. Qiu, and S. Shenker, *Phys. Rev. Lett.* **52**:1575 (1984).
38. H. N. V. Temperley and E. H. Lieb, *Proc. R. Soc. Lond. A* **322**:251 (1971).
39. M. P. Nightingale and H. W. J. Blöte, *J. Phys. A* **16**:L657 (1983).
40. M. P. Nightingale, *J. Appl. Phys.* **53**:7927 (1982).
41. B. Davies, *J. Stat. Phys.* **46**:535 (1987).
42. P. Reinicke, *J. Phys. A* **20**:5325 (1987).
43. P. Reinicke, Finite-size scaling functions and conformal invariance, preprint.
44. F. J. Wegner, *Phys. Rev. B* **5**:4529 (1972).
45. M. E. Fisher, *Rev. Mod. Phys.* **46**:597 (1974).
46. M. N. Barber, *Phys. Rep.* **29C**:1 (1977).
47. NAG routine F04ATF, Numerical Algorithms Group.